NASA CONTRACTOR REPORT

NASA CR-1511

ERROR SENSITIVITY FUNCTION CATALOG

by C. F. Martin and J. R. Vetter

Prepared by
WOLF RESEARCH AND DEVELOPMENT CORPORATION
Riverdale, Md.
for NASA Wallops Station

NATIONAL AERONAUTICS AND SPACE ADMINISTRATION • WASHINGTON, D. C. • MARCH 1970

NASA CR-1511

ERROR SENSITIVITY FUNCTION CATALOG

By C. F. Martin and J. R. Vetter

Prepared under Contract No. NAS 6-1467 by
WOLF RESEARCH AND DEVELOPMENT CORPORATION
Riverdale, Md.

for NASA Wallops Station

NATIONAL AERONAUTICS AND SPACE ADMINISTRATION

For sale by the Clearinghouse for Federal Scientific and Technical Information
Springfield, Virginia 22151 – Price $3.00

FOREWORD

The primary objective of the Error Sensitivity Function Catalog is to illustrate the effects of various systematic errors on orbital solutions involving range, range-rate, azimuth, and elevation observations.

The Catalog was written for the NASA Wallops Station GEOS-B C-Band System Project Group; therefore, the error effects have been determined specifically for the Wallops AN/FPQ-6 and other C-Band radars. However, the methods, analyses, and conclusions contained herein are of general interest, and should be applicable to many other orbital solutions involving range, range-rate, azimuth, or elevation observations.

TABLE OF CONTENTS

LIST OF FIGURES

LIST OF FIGURES (Cont'd)

LIST OF TABLES

SECTION 1.0
INTRODUCTION

An analysis of the performance capabilities of an instrumentation system, such as the AN/FPQ-6 radar, requires consideration of the manner in which the data is to be used. In tracking earth orbiting vehicles, trajectory data is normally processed in some procedure which attempts to obtain the most probable orbit, based on some assumptions as to the statistical properties of the measurement noise and the systematic errors affecting the determined orbit. An example of such a data reduction program is the NONAME data reduction program which uses the Bayesian least squares estimation technique to solve for a set of orbital elements and, optionally, certain coefficients producing systematic effects on either the measurements or on the integrated orbit.

Ideally, the result of the data reduction program will be an orbit which all measurements (after correction for biases, etc.) will fit exactly except for some error which will appear to be randomly distributed about the orbit. In addition, the data reduction program will produce an estimate of the orbital error due to this noise, although the measurement noise variances must be input to the program.

It is a well known fact, however, that residuals almost never even approach randomness, and that orbital error estimates based on measurement noise are notoriously low. It is also a well known fact that both of these discrepancies between theory and practice are due to the set of approximations which are made, and generally of necessity, in the actual usage of the Bayesian least squares

estimation procedure. Specifically, there are more unknowns affecting a general data reduction program than measurement noise and the set of parameters solved for. The presence of actual errors in such unknowns is exhibited in non-random residuals and errors in the orbital elements leading to errors in the orbit greatly in excess of that due to noise alone.

In general, the least squares estimation program will attempt to estimate all those parameters significantly affecting the orbit or measurements. But this capability is limited by a number of factors, including a limited amount of information in the actual data, limited computer storage and running time, and lack of knowledge as to which parameters actually have errors and are adversely affecting the solution.

It should be emphasized that the quality of the results of a data reduction is very strongly affected by the quality of the data input to the computer program. Data in this sense includes not just the actual set of measurements, as e.g. radar tracking data, but the complete set of parameters upon which the solution will be based. If there is a choice between using mission calibration (pre and/or post) of a radar to determine its biases, and solving for these biases in a data reduction program, the former course should always be followed -- assuming, of course, that comparable or better accuracies can be achieved. This amounts to nothing more than making use of all the information that is available and expecting to thereby obtain better results.

In practice, of course, the situation is not quite so clear cut. For example, if a radar can be calibrated such that its range bias is known to within 5 meters, there is the question as to whether better results will be obtained by solving for the remaining bias in the data reduction program or by ignoring it. In this example, the intuitive answer is that better results should be obtained by solving for the bias, since we are considering a Bayesian least squares data reduction. But this is not necessarily true when account is taken of the presence of other systematic effects which are always present. The general rule is that the more parameters that are adjusted, the larger will be both the noise only variance and the effects of errors in still unadjusted parameters.

The ORAN Program is designed to (among other things) complement an orbital data reduction program such as NONAME. As a data analysis tool, its primary advantage lies in the fact that it can compute in a single, relatively short, computer run the effects which numerous potential error sources would have on all quantities solved for in a particular data reduction, including orbital elements and measurement residuals. It is then possible to ascertain the sensitivity of a solution to a particular type of error and also see the pattern of the error reflected in the measurement residuals. With an estimate of the error in this parameter, a comparison with actual data reduction residuals can show whether this error source is negligible, or may be a potential explanation of the systematic trends in the measurement residuals.

There are several objectives which this report is intended to satisfy. They are:

A. To show the effects of systematic errors on data reductions using data from the Wallops FPQ-6 radar,

   a. as exhibited in measurement residuals

   b. as reflected in Bayesian least squares estimations of orbital elements and other adjusted parameters

   c. as reflected in orbital accuracy and in prediction capability.

B. To identify the systematic errors which most seriously degrade orbital accuracy.

C. To show the limiations of data reductions for error model coefficient recovery.

D. To demonstrate the utility of ESFC in data analysis.

The type of measurement model upon which the results of this report are based is discussed in Section 2 . In general, one or more FPQ-6 radars are assumed, with measurement noise levels corresponding to that which has been observed on data from the Wallops radar. Section 3 discusses the sources of unmodeled errors which are considered to be primarily responsible for total orbital error and systematic residuals.

In Sections 4 and 5, we attempt to meet objective A, first for a single station (Wallops) solution, and then with Wallops in a multi-station solution. Most of the significant error model terms are identified in these sections also, thus satisfying objective B. In Section 6, the problem of error model recovery is considered both for the single and multi-station solutions. Section 7 then demonstrates several means by which the ORAN program can be used to explain various aspects of the results of actual data reductions.

Section 8 summarizes some of the significant conclusions which can be drawn from the error analysis results discussed in this report. Appendix A presents--in a somewhat abstract form--the mathematical basis of the ORAN program. Simulated GEOS-B measurement rate and acceleration profiles as observed from the Wallops Island AN/FPQ-6 radar for two typical pass configurations are illustrated for reference in Appendix B.

SECTION 2.0
MEASUREMENT MODEL

The measurement model used in this analysis consists of radar slant range, range-rate and azimuth and elevation angles. Figure 1 illustrates the radar coordinate system, azimuth angle being measured from true north clockwise to the range vector and elevation angle being the included angle between the horizontal plane and the range vector.

For all arcs, the epoch orbital elements used were the differentially corrected position and velocity vectors obtained the the NONAME Data Reduction Program using actual AN/FPQ-6 measurements on GEOS-II. In general, all ORAN runs attempted to simulate actual tracking configurations, both in geometry and in time. In addition, all error propagations assumed a data reduction of the minimum variance type which could have been -- and in many cases was -- performed by NONAME.

The measurement noise values used in most of the ORAN runs discussed in this report are listed in Table 1 and are representative of the capabilities of the Wallops FPQ-6 radar. The range, azimuth, and elevation sigmas are the approximate noise levels which have been observed from NONAME reductions of short arc beacon track data on GEOS-II. These noise levels have been found to be appropriate (i.e., uncorrelated) for a sampling frequency at least as high as 1/second. Because of a sparcity of reduced range rate data from the Wallops radar, the range rate sigma used is a conservative estimate of the noise level based on the thermal noise equations.

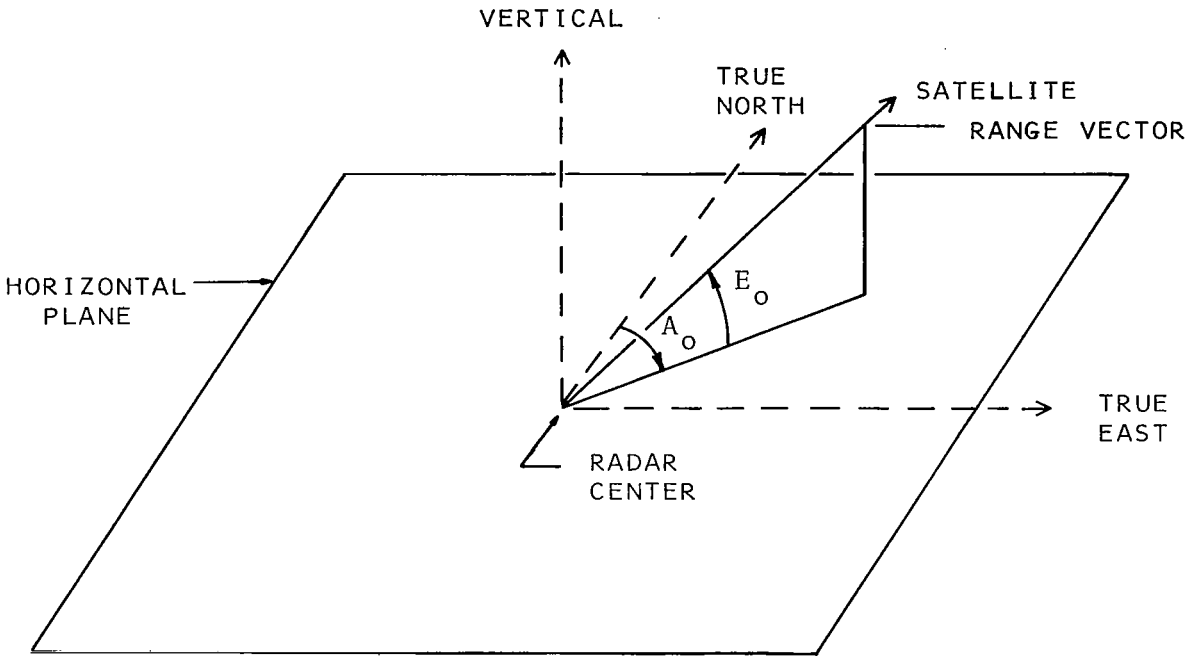

FIGURE 1

RADAR COORDINATE SYSTEM

TABLE 1

AN/FPQ-6 MEASUREMENT STANDARD DEVIATIONS

Measurement	One-Sigma Uncertainty
Range	5 meters
Range-rate	4 cm/sec
Azimuth	15 arc - sec
Elevation	15 arc - sec

Measurements uncorrelated, sampling rate = 1 per 15 seconds.

In ORAN, it is necessary only to simulate the geometry of a satellite pass; it is not necessary to use the same sampling rate as would be used in a data reduction. The propagation of the effects of unmodeled errors depends only upon relative measurement weights, and the propagation of modeled error effects scales as the inverse square root of the sampling frequency for fixed measurement weights. For computation efficiency, then, a sampling frequency of 1 point per 15 seconds was used in ORAN. To compare the ORAN modeled standard deviations with those of a data reduction with a sampling rate of 1 point/second, the ORAN sigmas should be multiplied by $\sqrt{1/T}$ where T is the sampling frequency. It will be found, however, that the modeled error contribution normally forms a small fraction of the total orbital error.

Unless cut off by time to simulate a NONAME data reduction, measurements were assumed to exist down to a radar elevation angle of 5 degrees. No measurements were allowed below this angle because of the difficulty in accurately correcting actual range and elevation data for tropospheric refraction in this region.

Figure 2 illustrates the relative geometry between selected GEOS-II satellite passes and the AN/FPQ-6 tracking stations at Wallops, Bermuda, Antigua and Patrick AFB. The first of these stations was used for all single station solutions considered in this report and all four stations were used for the multi-station solutions. The station geodetic coordinates are listed in Table 2.

To further indicate the tracking requirements on the FPQ-6 radar during GEOS-II passes, typical measurement rates and accelerations for two different passes over the Wallops AN/FPQ-6 sites are presented in Appendix B.

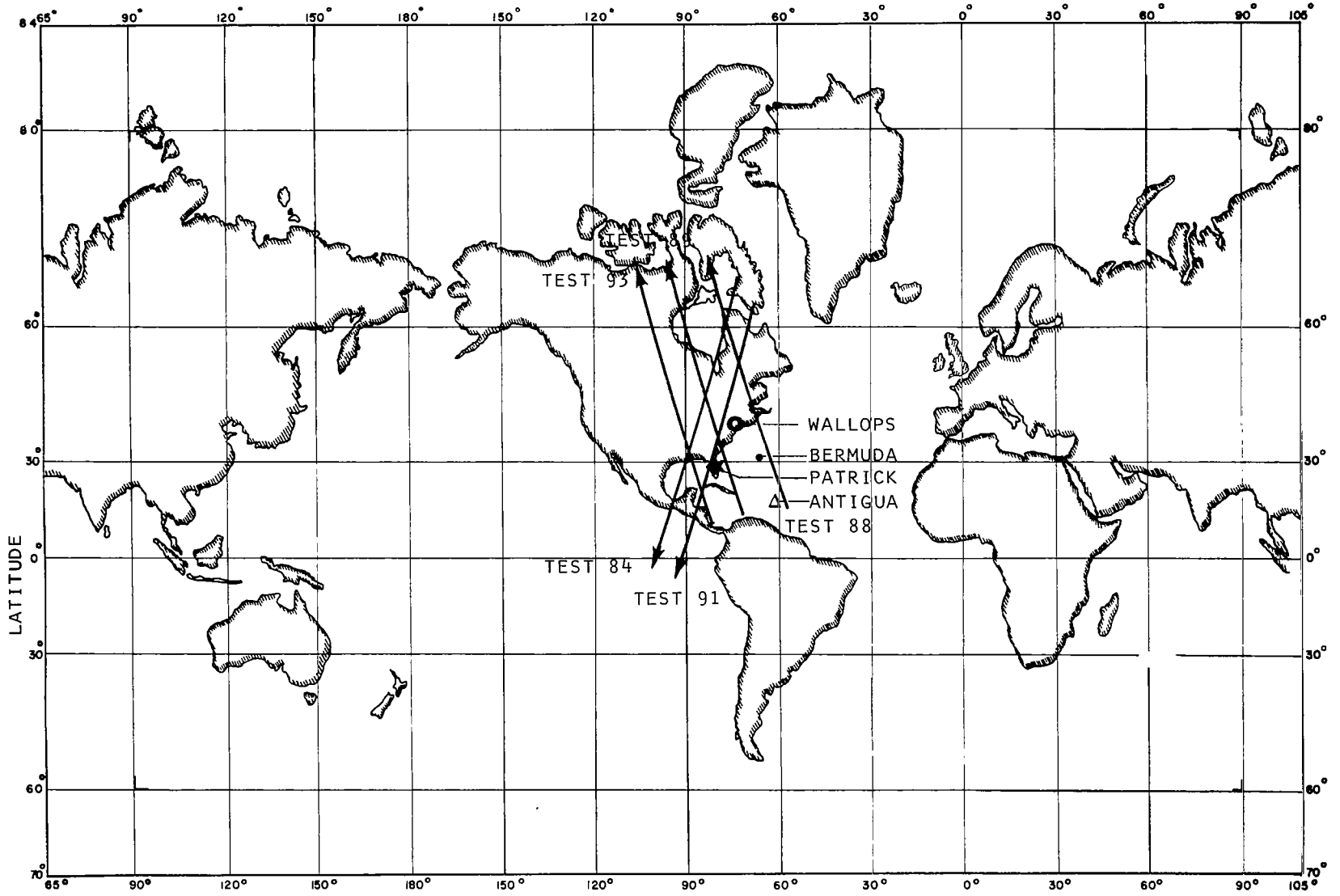

FIGURE 2 TYPICAL TRACKING GEOMETRY FOR GEOS-II ERROR ANALYSES

TABLE 2

SAO C-5 DATUM STATION POSITIONS

STATION	GEODETIC LATITUDE	EAST LONGITUDE	HEIGHT ABOVE ELLIPSOID (METERS)
Wallops Island (FPQ-6)	37°51'36".346	284°29'25".825	-40.504
ANTIGUA (FPQ-6)	17°08'37".372	298°12'24".796	+39.684
Patrick AFB (FPQ-6)	28°13'34".984	279°24'1".782	-36.40
Bermuda (FPQ-6)	32°20'51".95	295°20'46".24	+ 3.60

SECTION 3.0
SOURCES OF UNMODELED ERRORS

3.1 GENERAL

In very few instances, if ever, are raw measurements from any tracking instrument used in an orbit determination when the most accurate solution is desired. Instead, the measurements are first corrected as well as possible for all known systematic errors. (They may also be smoothed to reduce random errors.) In most cases, however, the corrections can only be made approximately, and systematic errors still remain of a magnitude larger than the actual "random" noise level on the measurements. One of the purposes of the ORAN program is to investigate the effects of incomplete or non-existent corrections for certain systematic errors on the measurements used in an orbital data reduction. Biases are the most obvious - and in most cases, the most important - example of an error of this type.

In addition to true measurement errors, actual orbit determinations are affected by two other major sources of error - station position errors and force field errors. Such errors enter the picture because of the nature of the orbit determination process - the best fit of calculated and observed (corrected) measurements. A calculated observation at a particular time depends upon the position of the station and the position of the satellite. Thus, station position errors enter the calculated measurement directly and force field errors enter because the satellite position at any time past epoch depends upon the force field used in integrating the orbit. The effects

on orbital data reductions of station position errors and certain force field errors can also be calculated by the ORAN program.

An assessment of whether or not a particular error source is really one of the more significant sources of error in an orbital solution requires more than just the form of the error as expressed by a tracker error model term. A reasonable best estimate or an upper limit for the expected error (or standard deviation) of the parameter is also required. Table 3 lists the uncertainty estimates for the set of parameters which have been considered for each radar used in ORAN runs discussed in this report. In general, the values chosen are close to being upper limits for expected errors, based on standard Wallops radar calibration procedures and current estimates of station position and force field errors. An indication of the source or procedure for obtaining the error model terms and their values as listed in Table 3 are given below.

3.2 INSTRUMENTATION ERRORS

3.2.1 Bias Errors

Errors of basically a bias type have been generally found to be the largest contributor to systematic error in radar tracking systems. An estimate of instrumentation bias errors can be obtained from pre- and post-mission calibrations. The range bias can be found by comparing a series of measured ranges to a fixed ground target with the surveyed range value. Similarly, the biases in azimuth and elevation angles can be determined by comparing a series of angle measurements to a boresight tower in both normal and plunge operation. The mean difference between the measured range and the sur-

TABLE 3

SOURCES OF UNMODELED ERRORS AND THEIR MAGNITUDES

UNMODELED ERROR	MAGNITUDE
Range Bias	5 meters
Range-Rate Bias	4 cm/sec
Azimuth Bias	50 arc-sec
Elevation Bias	50 arc-sec
Timing Error	50 μ sec
Elevation Droop	10 arc-sec
Mislevel Phase	10 degrees
Mislevel Amplitude	10 arc-sec
Velocity Servo Lag	100%
Acceleration Servo Lag	100%
Refraction Error	10%
Local Survey Error (X,Y,Z)	10 meters in each coordinate
Center of Mass Error (X,Y,Z)	20 meters in each coordinate
Geopotential Coefficient Errors (NWL5E-6-SAO M1 Diff)	100%
Gravitational Coefficient Error in μ=GM	1 ppm

veyed range is a measure of the bias in the range measurement and can be used accordingly as a pre-processing correction for range. Unfortunately, the calibration measurements must normally be made at a very low elevation angle within the atmosphere and in the near field pattern of the antenna; since multipath and tropospheric refraction effects on the calibration process are both somewhat uncertain and variable, the residual biases after calibration may be considerable.

Presently, the preprocessing procedures for the Wallops AN/FPQ-6 radar apply a range bias correction obtained from the pre- and post-mission calibrations, but do not apply angle bias corrections. The bias values listed in Table 3 are consistent both with expected residual calibration errors and with the results of analyses performed on data taken during collocation tests at Wallops.

3.2.2 Refraction Errors

The tropospheric refraction correction applied to Wallops radar data during preprocessing uses a measured surface index of refraction and a cosecant dependence upon elevation angle. A refraction correction based upon the ray path integration using a measured vertical refractive index profile has an expected error on the order of 2 -4% [1]. The use of a correction procedure based upon a surface index only should introduce a few percent additional error, as should the flat earth approximation (i.e., the csc E dependence). Taking into account the fact that the location of the radar near the land-sea boundary where atmospheric conditions are quite difficult to predict, a residual refraction error of 10% of the correction is an approximate upper limit to the error which could be expected.

3.2.3 Hardware-Oriented Errors

On-site radar calibration generally removes a major portion of all hardware-oriented errors such as droop, mislevel, non-orthogonality, etc. However, after the calibration corrections are applied, a small residual error still remains which acts as a bias on the measurements. Moreover, the calibration constants which are used in the computations are determined only periodically, so that any variations in the radar set-up procedures, changes in instrumentation or the daily use of the equipment may affect their value. Mislevel experiemnts conducted on the Wallops AN/FPQ-6 pedestal during a 24 hour period in July 1968 with clinometer readings taken every hour showed a variation in mislevel of 7 degrees in phase and 7.5 arc-sec in amplitude. For this study, a more conservative estimate of 10^{o} in phase and 10 arc-sec in amplitude was used as an estimate of the unmodeled mislevel errors. Previous experience with antenna sag of the Cassegranian dish of the AN/FPQ-6 radar showed that 10 arc-sec was a reasonable value for measurement uncertainty in elevation droop angle. In addition, because the radar was, by choice, not operated in a mode to correct the raw radar data for dynamic lag in the azimuth and elevation servo loops, an unmodeled error for both velocity and acceleration servo lag of 100% was assumed.

3.3 TIMING ERRORS

At Wallops Station, a master clock generates coded timing pulses which are transmitted by telephone lines to the AN/FPQ-6 radar. Diurnal variations are measured and

recorded daily at the master site by direct comparison of the master oscillator and the cesium beam standards. This variation can range from 50 to 300 μ sec and is not normally accounted for in the pre-processing. A value of 50 μ sec was used as an estimate of the unmodeled timing error for all radar sites.

3.4 STATION POSITION ERRORS

The orbit prediction process predicts the position of a satellite in an inertial coordinate system by relating the satellite to known points in a local (radar-centered) coordinate system. Consequently any error in the position of the reference points will degrade the prediction accuracy. The best determinations from satellite motion have recovered station positions to 15 meters with respect to the geocenter [2]. In fact, references [3] and [4] state that the center of mass coordinates of any SAO C-5 Baker-Nunn stations have been assessed to have approximately 15 - 20 meter accuracy.

A ground survey of the Wallops AN/FPQ-6 site conducted in March 1968 by the STADAN Operations Division, NASA/GSFC, has a positional uncertainty with respect to the Jupiter, Florida Baker-Nunn station of less than 6 meters. Transformed to the geocenter, the positional uncertainty for the Wallops Site is less than 21 meters. For the purposes of this report, the uncertainties in the X, Y, Z position of center of mass coordinates have been assumed at 20 meters each, while 10 meters has been assumed for the position uncertainties for each X, Y, Z position of the Wallops FPQ-6 site.

Since all stations utilized in this study (and utilized in Wallops data reductions) are positioned on the SAO C-5 Datum, they all have a comparable positional uncertainty with respect to the geocenter. For simplicity, all stations were also assumed to have the same topocentric position uncertainty.

3.5 FORCE FIELD ERRORS

At the altitude of the GEOS-II satellite, atmospheric drag forces are negligible. Since the perturbations due to the sun and moon can be quite accurately modeled in the orbit generation process, the only significant force field errors are those in the earth's gravitational coefficient and its harmonic coefficients.

3.5.1 Gravitational Coefficient

The best estimate of the gravitational constant, $GM_{\oplus}$, has been obtained from the reduction and analysis of Ranger Lunar Radio Tracking Data by JPL. The uncertainty in their determination is $\pm 1 \times 10^{-6}$ [5]. This value was carried as an unmodeled error in all simulations.

3.5.2 Geopotential Coefficients

Because significant variations exist for the geopotential coefficients recovered from terrestrial and/or satellite tracking data - differences which are generally much greater than the quoted standard deviations - a scheme has been adopted which utilizes the difference between the best determined gravity models as the effec-

tive uncertainty in the total set of gravitational harmonics. In this manner, any fractions of this difference can be represented in the solution as an unmodeled error.

Assuming the existence of more than one gravity model of comparable accuracy and that these models do not have too much common ancestry, this appears to be the most valid representation of the total geopotential coefficient errors. The most accurate unclassified geopotential models are considered to be the SAO M1, the APL 3.5, and the NWL 5E-6. Differences between any two of these three models are available in the ORAN program as a representation of the geopotential coefficient error. Data reductions with the NONAME program are normally done using the SAO M1 gravity model, which has been shown to provide better long arc orbital fits than either of the other two. Most of the ORAN runs considered in this report used 100% of the differences between the SAO M1 and the NWL 5E-6 models as the geopotential coefficient error. Since the SAO model is known to be a more accurate model, this results in a somewhat pessimistic estimate of the effects of geopotential coefficient errors.

SECTION 4.0
UNMODELED ERROR EFFECTS ON WALLOPS SINGLE STATION SOLUTIONS

4.1 SINGLE STATION SHORT ARC

An error analysis of the unmodeled error effects (Table 3) on Wallops FPQ-6 measurements of GEOS-II was conducted for two single pass soultions. Collocation test numbers 84, 89 and 54 were chosen for this study as representing, respectively, a low elevation, a moderate elevation and a high elevation pass configuration. Test 84 attains a maximum elevation angle of 23 degrees; test 89 attains a maximum elevation angle of 63 degrees; and test 54 attains a maximum elevation angle of 84 degrees.

4.1.1 Orbit Accuracy

The estimated effects of the unmodeled errors on the orbit at epoch are given in Table 4 for test 84, Table 5 for test 89, and Table 6 for test 54. The estimates are presented as errors in the H, C, and L orbit coordinate system. The H and L coordinates lie in the orbit plane formed from the radius and velocity vectors. The H, or radial, direction lies along the radius vector. The L, or along track direction, is in the orbit plane perpendicular to the radius vector and has a component along the positive velocity direction. (For circular orbits, L is along the velocity vector.) The C, or cross track, direction is perpendicular to the orbit plane.

The measurement noise contribution to the orbital error is presented across the top row of Table 4; the bottom row gives the total root sum square (rss) contribution of measurement noise and all unmodeled errors. These tables show that the unmodeled errors propagate into large errors in the epoch elements. This is particularly evident for refraction, the instrument biases and hardware errors.

It should be noted that the local survey unmodeled errors are redundant for the single station solution. This is due to the fact that the local survey is merely a transformation of the center of mass system. This statement can be verified by comparing the rss values of the local survey orbit errors with the center of mass errors; the agreement is excellent, clearly showing the scaling factor of 2 between the two sets of errors (see Table 3).

The effects of the unmodeled errors on total rss orbit accuracy are presented in Figure 3 for test 84, test 89 and test 54 as a function of time from epoch. In addition, Figure 4 illustrates the contribution of instrumentation bias errors towards orbit degradation and shows that the angle bias errors are the dominant error source towards orbit inaccuracies. It is apparent that the orbit accuracy is improved by almost a factor of two during the data span for higher elevation passes. At the beginning of the next revolution, the orbit accuracy would have improved almost as significantly as during the first orbit through the data span. The orbit error is reduced on the next revolution because it passes through the same inertial position that was used in determining the initial orbit.

TABLE 4

SINGLE STATION LOW ELEVATION SHORT ARC SOLUTION (TEST 84)

ESTIMATED HCL ERROR ON EPOCH ELEMENTS DUE TO UNMODELED PARAMETERS

DELTA H (METERS)	DELTA C (METERS)	DELTA L (METERS)	DELTA HDOT (CM/SEC)	DELTA CDOT (CM/SEC)	DELTA LDOT (CM/SEC)	UNADJUSTED PARAMETER
25.52	33.67	23.49	4.55	6.60	1.51	NOISE
-3.76	-1.62	-4.93	3.68	0.16	2.05	NWL-SAO GRAV
207.04	-495.18	-193.51	13.31	68.57	-0.99	REFRACTION
-2.17	-5.94	-6.90	0.65	-0.56	-0.05	WALLOPS X
2.03	7.16	-8.12	0.55	-0.20	0.01	WALLOPS Y
9.53	-2.30	4.37	-0.49	-0.16	-0.30	WALLOPS Z
-1.06	-14.61	-9.15	0.90	-1.08	-0.21	C.O.M. X
-13.24	9.05	-19.79	1.73	-0.28	0.44	C.O.M. Y
14.90	8.49	-7.46	0.27	-0.51	-0.36	C.O.M. Z
-3.65	-4.02	1.26	0.29	-0.05	-0.46	RANGE BIAS
-24.73	23.02	-13.63	9.25	-7.93	4.07	R RTE BIAS
-530.53	472.19	-155.22	31.79	9.37	-0.90	ELEVN BIAS
9.48	680.00	560.27	-55.18	-162.12	4.87	AZMTH BIAS
0.04	-0.10	-3.57	0.32	-0.02	0.00	TIMING
-96.02	85.49	-28.04	5.69	1.75	-0.19	EL DROOP
17.60	-56.66	-29.02	4.81	6.48	1.16	MISLEVEL
-58.82	40.69	-26.93	5.29	2.87	0.27	MSLVL PHSE
-0.64	-16.66	-14.24	1.66	3.79	0.02	VEL SRV LAG
1.16	-0.91	0.44	-0.09	-0.04	-0.00	ACC SRV LAG
582.41	972.20	615.98	66.65	176.77	7.11	TOTAL ERROR

TABLE 5

SINGLE STATION MEDIUM ELEVATION SHORT ARC SOLUTION (TEST 89)

ESTIMATED HCL ERROR ON EPOCH ELEMENTS DUE TO UNMODELED PARAMETERS

DELTA H (METERS)	DELTA C (METERS)	DELTA L (METERS)	DELTA HDOT (CM/SEC)	DELTA CDOT (CM/SEC)	DELTA LDOT (CM/SEC)	UNADJUSTED PARAMETER
9.76	27.40	8.92	2.80	6.61	0.86	NOISE
-1.44	0.48	-1.40	0.32	-0.84	0.05	NWL=SAO GRAV
8.34	44.89	-7.18	3.41	1.40	1.44	REFRACTION
-0.67	8.51	-3.35	0.24	0.48	0.01	WALLOPS X
-0.67	4.79	10.66	-0.81	-0.54	0.07	WALLOPS Y
9.93	0.42	3.14	-0.35	0.15	-0.24	WALLOPS Z
2.83	15.17	-8.52	0.58	1.16	-0.10	C.O.M. X
-16.31	9.30	6.18	-0.30	-0.62	0.45	C.O.M. Y
11.12	8.08	20.69	-1.72	-0.66	-0.18	C.O.M. Z
-3.30	3.76	2.98	-0.46	-0.58	-0.77	RANGE BIAS
-23.27	-22.02	-23.19	9.03	6.61	2.68	R RTE BIAS
-78.18	-258.20	-1.59	-3.26	2.86	-1.90	ELEVN BIAS
-10.91	523.45	-157.25	20.35	-170.50	-7.21	AZMTH BIAS
-0.10	0.25	-3.63	0.33	-0.01	-0.00	TIMING
-8.92	-32.84	1.01	-0.95	0.00	-0.41	EL DROOP
24.54	37.47	13.96	-2.99	5.33	-0.06	MISLEVEL
4.09	-50.14	19.66	-5.01	10.75	-0.59	MSLVL PHSE
-2.12	18.69	-7.78	1.69	-5.28	0.06	VEL SRV LAG
2.55	6.78	0.61	-0.15	-0.17	-0.01	ACC SRV LAG
90.32	591.43	163.52	23.84	171.30	8.19	TOTAL ERROR

TABLE 6

SINGLE STATION HIGH ELEVATION SHORT ARC SOLUTION (TEST 54)

ESTIMATED HCL ERROR ON EPOCH ELEMENTS DUE TO UNMODELED PARAMETERS

DELTA H (METERS)	DELTA C (METERS)	DELTA L (METERS)	DELTA HDOT (CM/SEC)	DELTA CDHOT (CM/SEC)	DELTA LDOT (CM/SEC)	UNADJUSTED PARAMETERS
7.40	29.50	6.20	2.08	6.37	0.60	NOISE
-4.05	5.94	-2.20	1.49	-1.95	0.42	NWL-SAO GRAVITY
0.00	-3.16	-1.62	0.18	0.24	0.23	REFRACTION
0.67	9.46	-4.01	0.26	0.17	-0.03	WALLOPS X
-0.88	1.35	10.03	-0.79	0.55	0.15	WALLOPS Y
10.18	-0.22	4.25	-0.61	0.01	-0.26	WALLOPS Z
5.60	17.82	-8.97	0.50	0.17	-0.20	CT. MASS. X
16.28	6.58	2.66	0.13	0.72	0.55	CT. MASS. Y
11.10	1.86	21.67	-2.00	0.87	-0.08	CT. MASS. Z
-5.82	-0.90	2.35	0.39	0.15	-0.64	RNG. BIAS
-22.71	15.20	-19.10	6.70	-3.22	1.91	RRATE BIAS
-0.17	21.17	1.69	-0.65	-0.59	-0.11	ELV. BIAS
-12.54	759.87	67.82	0.03	-168.72	-6.22	AZM. BIAS
-0.10	0.26	-3.72	0.35	-0.01	0.00	TIMING
0.11	2.25	0.26	-0.11	-0.15	-0.02	ELV. DROOP
-0.77	64.06	6.78	-1.36	0.35	-0.51	MISLEVEL
22.05	45.41	23.27	-6.57	-11.17	-2.44	PHASE
-9.03	-22.85	-10.03	2.75	5.12	1.04	VEL. SRV. LAG
3.30	-32.58	-1.04	-0.10	-0.93	-0.01	ACC. SRV. LAG
43.38	776.30	80.11	10.49	169.34	7.15	TOTAL ERROR

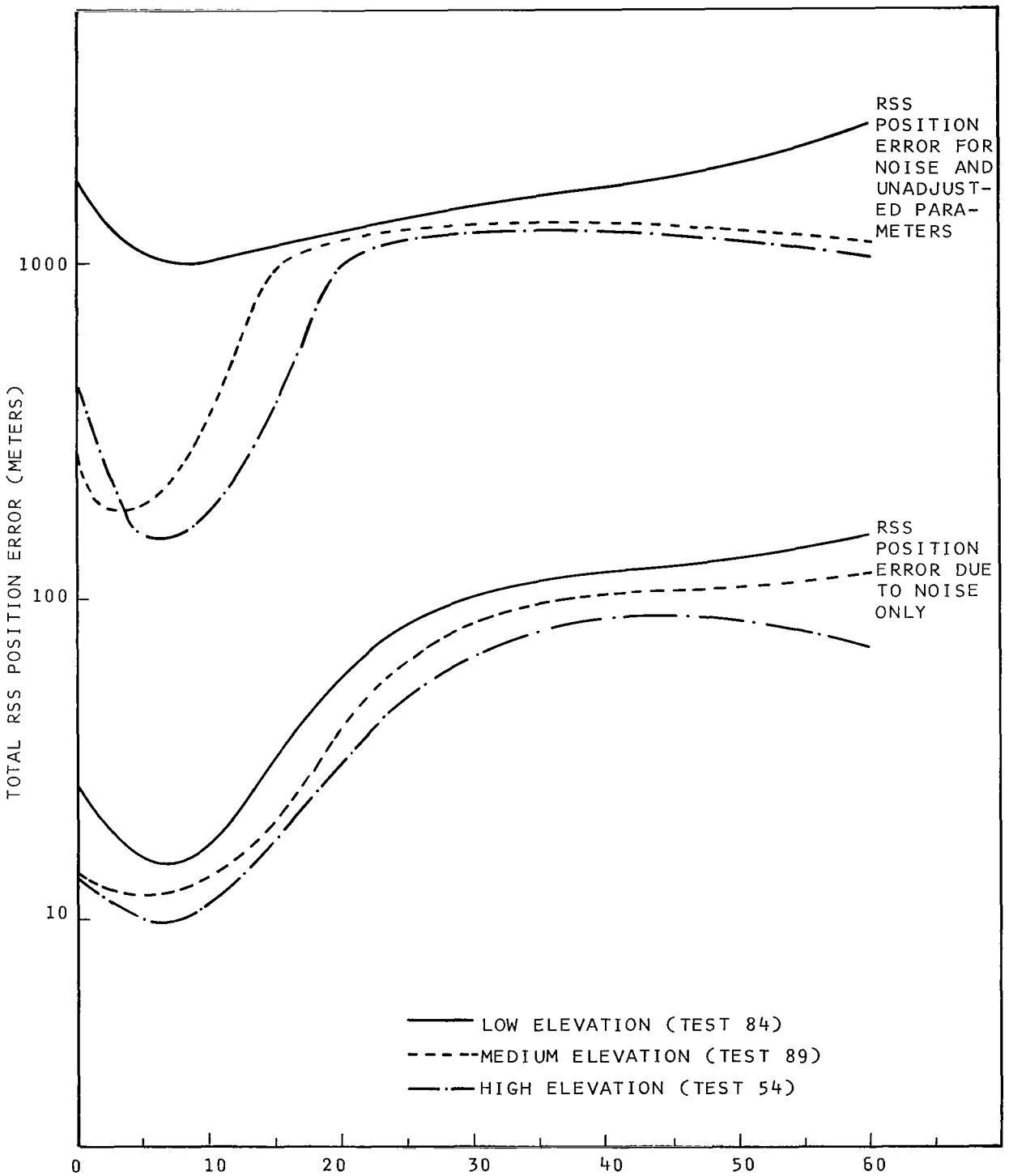

FIGURE 3 TOTAL ORBIT ACCURACY ON SHORT ARC PASSES

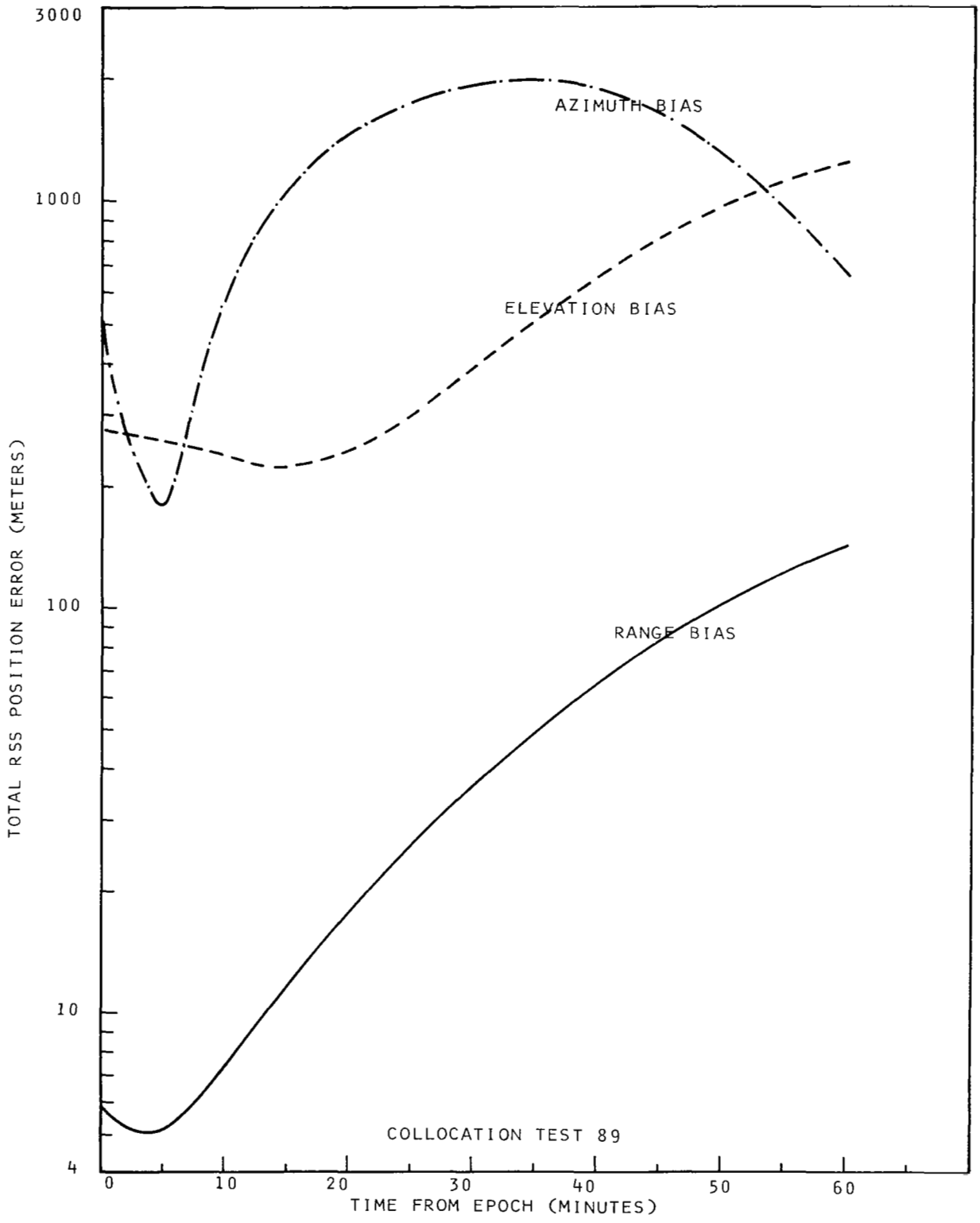

FIGURE 4 TOTAL ORBIT ACCURACY ON TYPICAL MEDIUM ELEVATION PASS SOLUTION FOR UNADJUSTED MEASUREMENT BIAS ERRORS

4.1.2 Residuals

The effects of the most significant unmodeled errors on the measurement residuals are presented in Figure 5 for test 84, Figure 6 for test 89, and Figure 7 for test 54. The figures show that the elevation bias and refraction is clearly the dominant error source on the range, azimuth and elevation measurement residuals. At very high elevation angles, the elevation bias gets propagated into a nearly constant bias in the elevation residuals; at low elevations its effects are still systematic but greatly reduced. The effect of a range bias on the residuals is relatively insignificant since most of it is absorbed into the orbit (see Section 4.1.1); this is also the case for an azimuth bias. However, although a large portion of an elevation bias is absorbed into the orbit, it nevertheless still has a relatively large systematic effect on the measurement residuals, at least for short-arc solutions.

From the curves shown in Figures 5,6,and 7 for the effects of azimuth and elevation biases on azimuth and elevation residuals, it will be seen that of the approximately 52 arc-sec assumed for each bias, almost all of the azimuth bias and about 30 arc-sec of the elevation bias are absorbed by the orbit for both the medium and low elevation passes. That a large effect from each bias has been propagated into the orbit is clearly shown in Figure 4. We thus see that, particularly in the short-arc case, the magnitudes of residuals is not necessarily an indication of orbital accuracy, since the orbit can act as a low pass filter and absorb a large portion of the systematic error in the measurements of a tracking system. In the next section we will see that measurement systematic errors are less readily absorbed by the orbit in a long arc reduction.

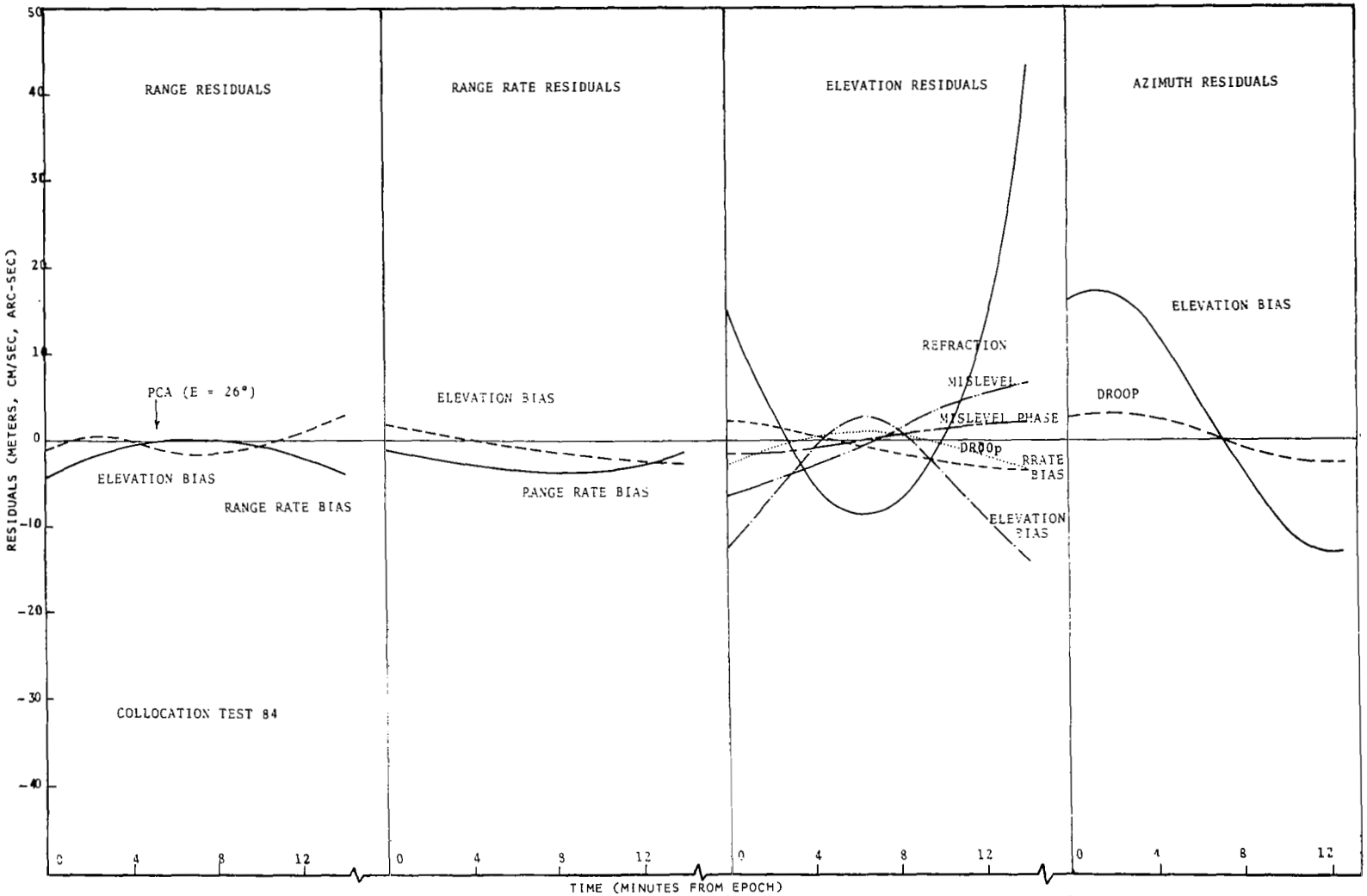

FIGURE 5 MAJOR UNMODELED ERROR EFFECTS ON WALLOPS ISLAND AN/FPQ-6 MEASUREMENT RESIDUALS FOR TYPICAL LOW ELEVATION PASS

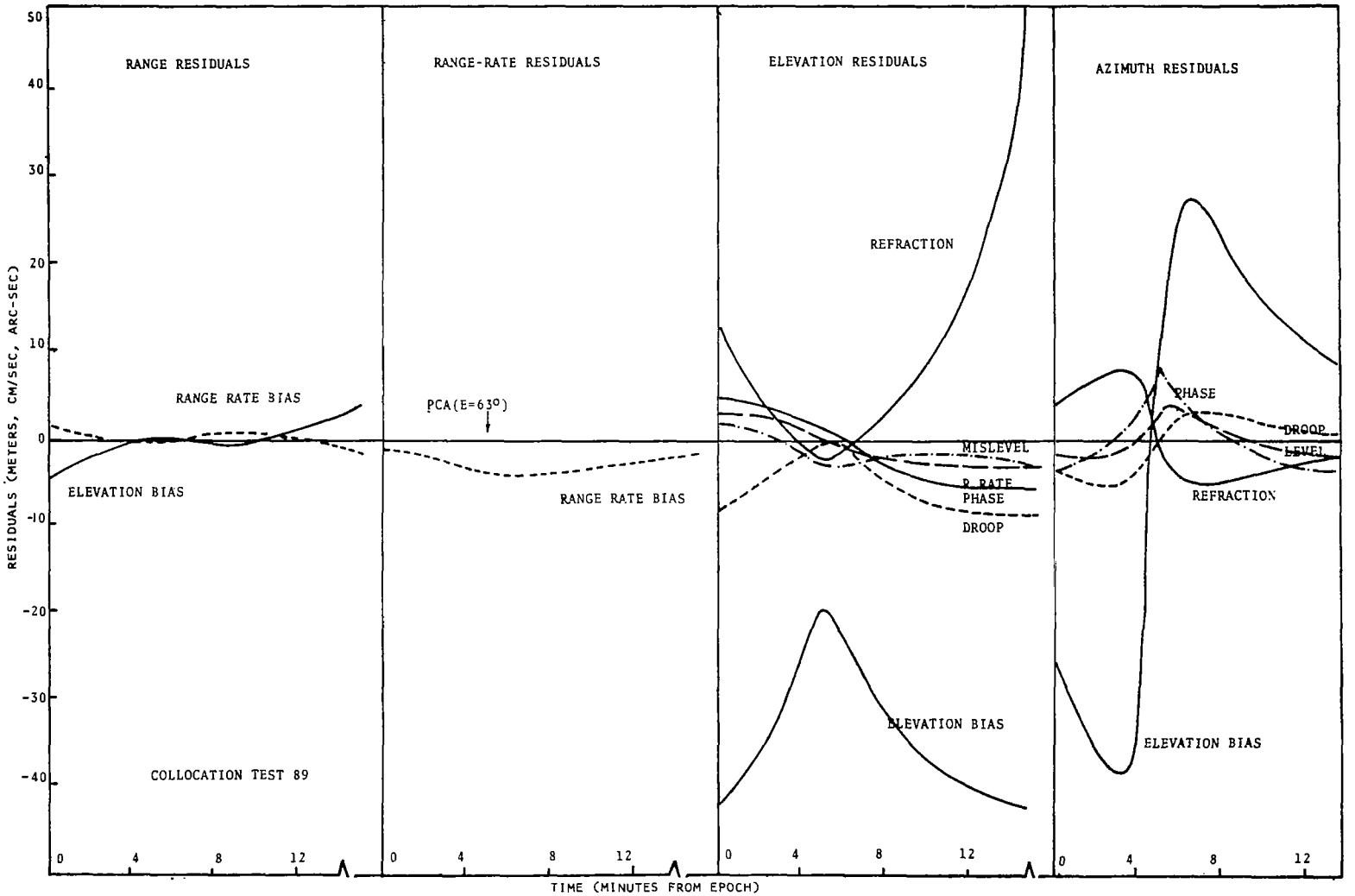

FIGURE 6 WALLOPS ISLAND AN/FPQ-6 MEASUREMENT RESIDUALS FOR TYPICAL MEDIUM ELEVATION PASS

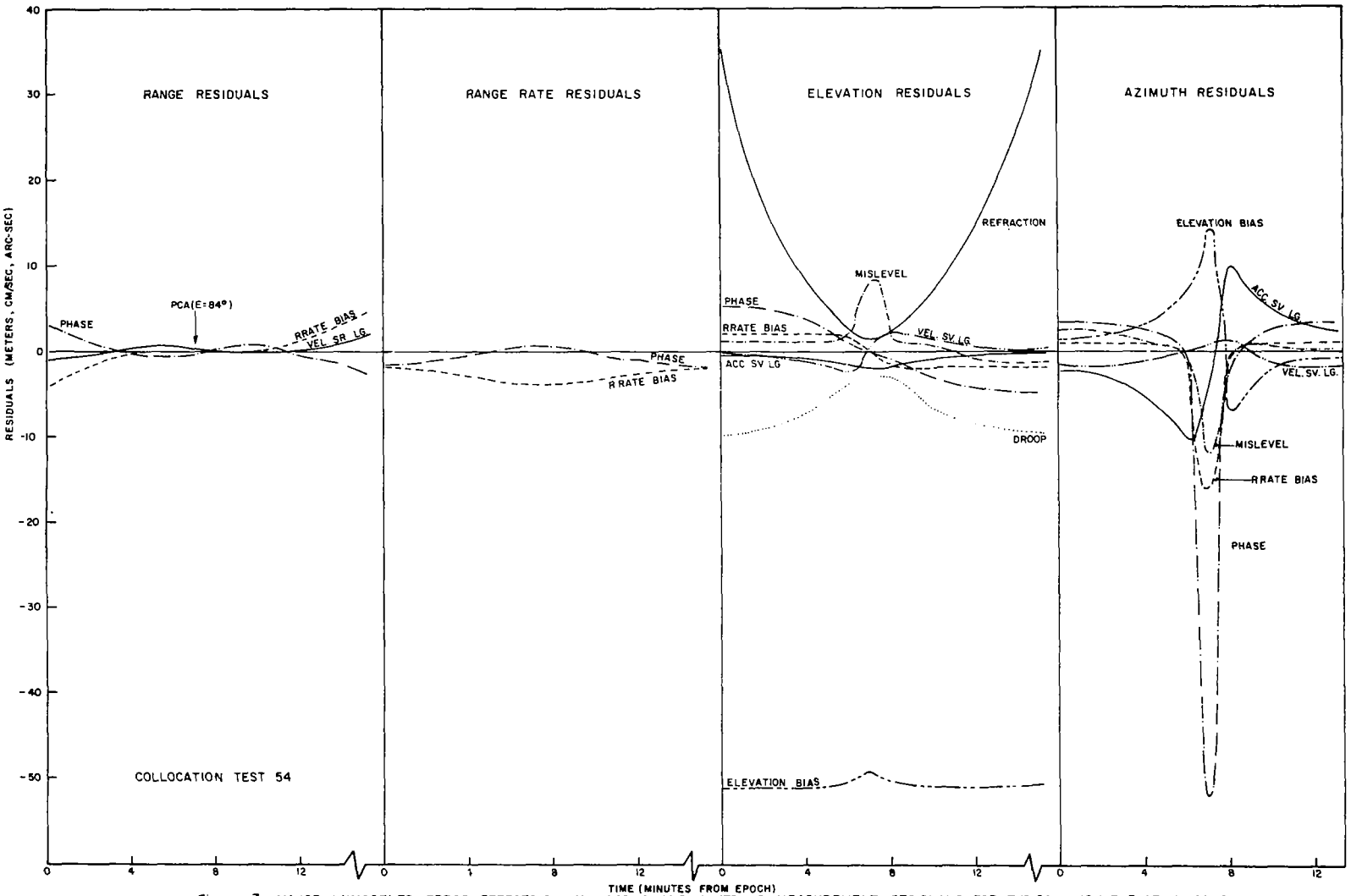

Figure 7 MAJOR UNMODELED ERROR EFFECTS ON WALLOPS ISLAND AN/FPQ-6 MEASUREMENT RESIDUALS FOR TYPICAL HIGH ELEVATION PASS

4.1.3 Characteristics of Short Arc Solutions

The results of the low and high elevation short arc passes have indicated that:

a. Instrumentation biases do not show up as true biases on the measurement residuals, but are largely absorbed by the orbit.

b. Biases in azimuth, elevation and refraction are the dominant error sources.

c. The effects of a timing bias, survey and geopotential errors on the residuals are negligible in comparison with bias errors.

4.2 LONG ARC SINGLE STATION

In this section, we consider the ORAN computations for a typical 24 hour arc with tracking by the Wallops FPQ-6 on 3 GEOS-II passes. Runs were also made for a 48 hour arc but the results did not differ in any significant respects from the one day arc and for that reason will not be separately discussed. Certain aspects of a 48 hour arc are, however, considered in Section 7.2.

The tracking times for Wallops for the 3 different passes are shown on Figure 8. All 3 passes are relatively high elevation passes, and correspond to collocation test numbers 89,91, and 93. It will be noted from Figure 2 that, geometrically, passes 1 and 3 are very similar, but quite different from pass 2. This fact is very significant and will be discussed below.

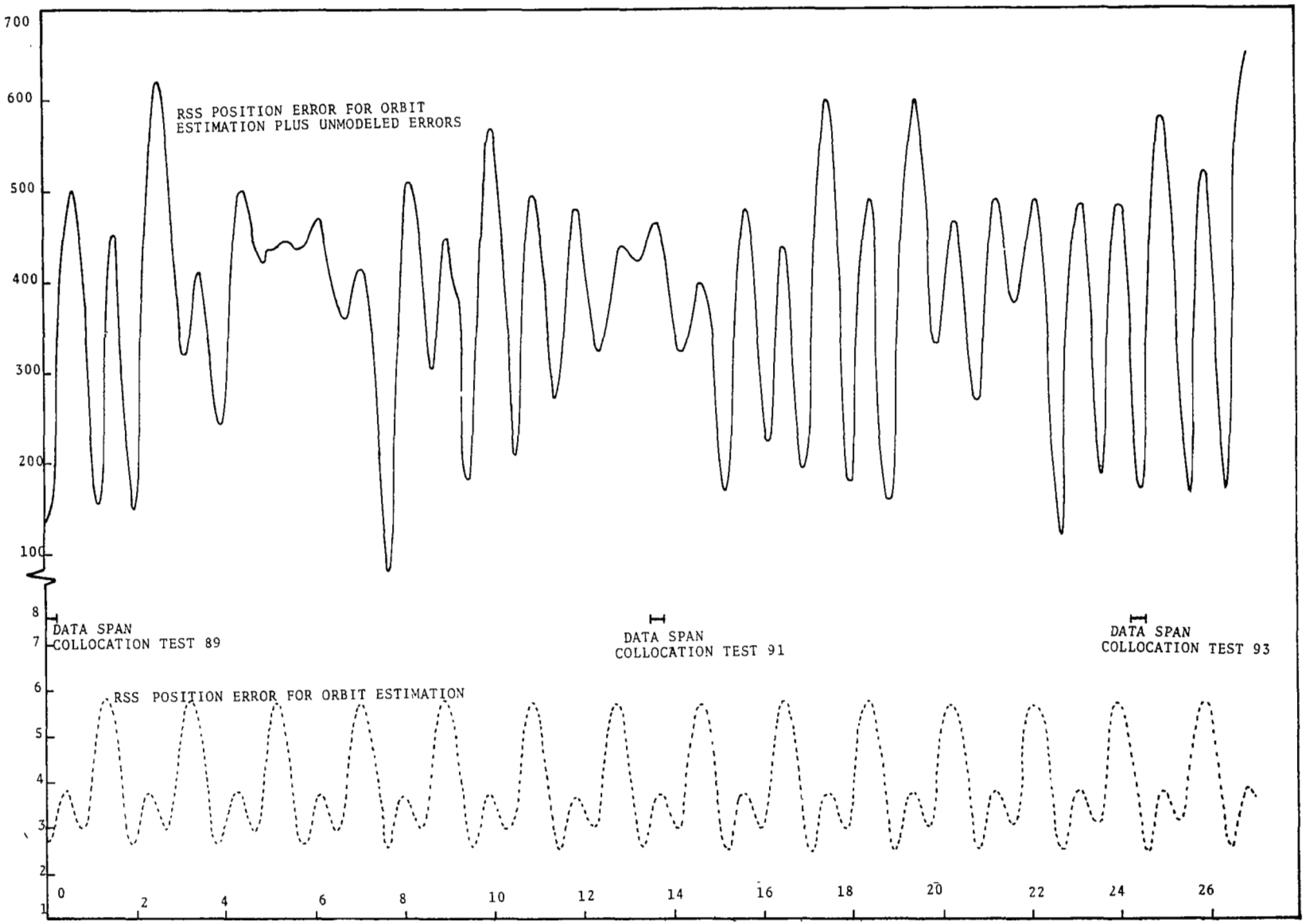

FIGURE 8 TOTAL RSS POSITION ERROR FOR SINGLE STATION ONE DAY LONG ARC SOLUTION

4.2.1 Orbit Accuracy

Considering the noise only contribution, the accuracy of the epoch elements which can be obtained by the 3 passes of radar data is shown in the first row of Table 7. It will be noted that the numbers are much smaller than the corresponding sigmas for the single pass solutions. Basically, the multi-revolution solution has to be much better than the single pass solution because the orbital period is much better determined.

Let us now consider the time propagation of the noise only variance covariance matrix, as is shown by the lower curve of Figure 8. As was noted above, two of the three passes, upon which the orbital solution is based, are quite similar geometrically. Stated otherwise, this means that the satellite is viewed by these passes in the same portion of the satellite's inertial trajectory and from similar viewing angles. Since we already know from the single pass solution that the orbital accuracy has a minimum each revolution (starting with the tracking period) we would expect that with data from these two similar passes, we would still have just one minimum per revolution. The minimum would, of course, be much deeper because of the better period determination.

The middle tracking period (actually, the fact that it is the middle rather than one of the end periods is probably irrelevant), however, complicates matters because it occurs near the time at which the orbital uncertainty would otherwise be a maximum. The net result is, as is clearly shown in Figure 8, that the overall orbit has a near minimum for the two similar passes, and a local maximum for the middle pass. The true maximum has, however, been shifted to another portion of the orbit.

TABLE 7

SINGLE STATION ONE DAY LONG ARC SOLUTION (TESTS 89, 91, 93)

ESTIMATED HCL ERROR ON EPOCH ELEMENTS DUE TO UNMODELED PARAMETERS

DELTA H (METERS)	DELTA C (METERS)	DELTA L (METERS)	DELTA HDOT (CM/SEC)	DELTA CDOT (CM/SEC)	DELTA LDOT (CM/SEC)	UNADJUSTED PARAMETER
1.27	1.70	1.67	0.18	0.32	0.11	NOISE
-0.09	-1.31	0.44	-0.02	0.01	0.01	REFRACTION
1.24	17.14	-0.82	-0.05	-0.58	-0.11	RANGE BIAS
-0.19	-0.82	-2.81	0.25	-0.07	0.01	R RTE BIAS
-2.18	-1.64	-3.50	0.33	-0.67	0.19	AZMTH BIAS
2.68	-4.97	-3.16	0.35	-0.36	0.24	ELEVN BIAS
-0.58	-17.30	10.24	-0.78	0.16	0.08	C.O.M. X
2.18	-43.02	-6.11	-0.03	3.17	-0.20	C.O.M. Y
-3.75	8.46	-22.16	1.00	-1.51	0.32	C.O.M. Z
67.60	187.08	-5.22	7.52	-33.51	-7.14	NWL-SAO GRAV
2.42	6.43	-0.68	0.09	-0.37	0.27	GRAV COEF
67.90	193.92	23.36	7.65	33.71	7.17	TOTAL ERROR

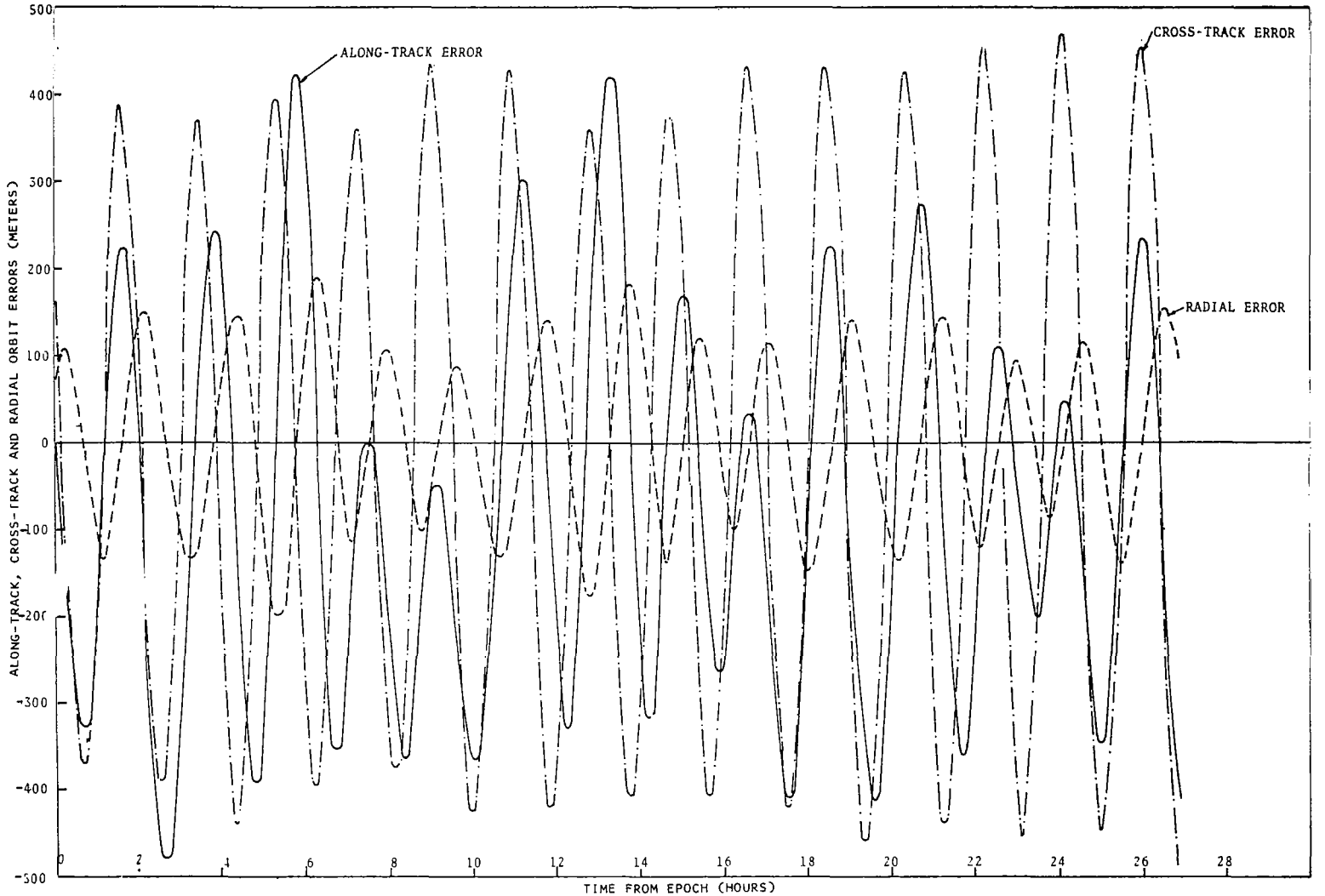

FIGURE 9 ALONG TRACK, CROSS TRACK AND RADIAL ORBIT ERRORS DUE TO NWL-SAO GRAVITY MODEL DIFFERENCES - ONE DAY LONG ARC SOLUTION

The effects of the unmodeled error complement on the epoch elements are also shown in Table 7. The most striking error source is that due to errors in the geopotential field. By comparison, all other parameters have effects which are almost negligible. When the effects of all the unmodeled parameters are added (in an rss manner) to the noise only sigmas, the total epoch element uncertainty is given in the last row of Table 7. Again we see, except in an even more dramatic manner, that the noise only contribution to the total orbit error is only a small fraction of the total error.

The propagation of the total variance covariance matrix into orbital error is shown in the top curve of Figure 8. From Table 7, we know that this curve is due to predominantly geopotential coefficient errors. To shed some light on the rather peculiar behavior of the total accuracy curve, we show in Figure 9 the individual radial, cross track, and along track components of the geopotential error effects. As expected, they are near - but not quite - sinusoids with the period of the orbit. There is both some amplitude and some phase modulation in all components. That the root sum of squares of the curves in Figure 9 does indeed effectively produce the top curve of Figure 8 may be readily verified.

Several distinct features may be observed about the total orbital accuracy:

a. It has two maxima and two minima per orbital period and these maxima and minima occur at the same times as they do in the bottom curve of Figure 8 for the noise only situation.

b. Minima occur during both the first and third passes.

c. A local maximum occurs during the second pass.

It thus is seen that the modeled and modeled + unmodeled cases have a number of characteristics in common. It now remains only to explain the peculiar features of the geopotential coefficient error effects. In simplest terms, the explanation is the following.

If geopotential coefficient errors exist in a data reduction, and no special provision is made for solving them or their effects, the least squares process has no choice but to arrive at a set of orbital elements (and perhaps other parameters) which do their best to minimize the weighted sum of squares of measurement residuals. Needless to say, this set of elements will be different from what they would have been had geopotential coefficient errors not been considered. As calculated by ORAN, the errors in the epoch orbital elements are shown below for the tracking and data reduction configuration being considered in this section - assuming, of course, that the differences between Smithsonian and Naval Weapons Lab gravity models provide a true representation of the geopotential coefficient errors. In Keplerian element form, these differences are:

$\delta a = -14.887$ m
$\delta e = 13.507 \times 10^{-6}$
$\delta i = 7.268''$
$\delta T = 19.515 \times 10^{-3}$ seconds
$\delta \Omega = 8.647''$
$\delta \omega = -40.202''$
$\delta M = 38.252''$

So errors in geopotential coefficients get propagated as much as possible into the epoch elements. However, epoch elements do not by themselves determine the orbit for all future times. The force model again enters the picture, and therein lies the explanation for the peculiar behavior of the curves in Figure 9 and the top curve in Figure 8. They have one contribution due to changes in the epoch Keplerian elements, but this contribution must have the period of the orbit as its basic period. The other contribution is a direct orbit generation type effect in which all the geopotential coefficients have effects according to their "natural" frequencies.* On this basis, the top curve as shown in Figure 8 should be the sort of total error behavior that would be expected.

4.2.2 Residuals

The propagation of the most significant unmodeled errors into the measurement residuals is shown in Figure 10. As expected from their effects on the epoch elements, the geopotential coefficient errors propagate into large measurement residuals. For range and range rate, such errors are by far the dominant contributor to systematic residuals. However, for azimuth and elevation measurements the biases on the respective measurements are the most significant contributors to residual effects.

---

* Though perhaps not obvious, the predominant periodicities of all geopotential coefficients is once per revolution (to which is added an m times daily effect, where m is the order of the harmonic). The different coefficients have widely varying phases, of course.

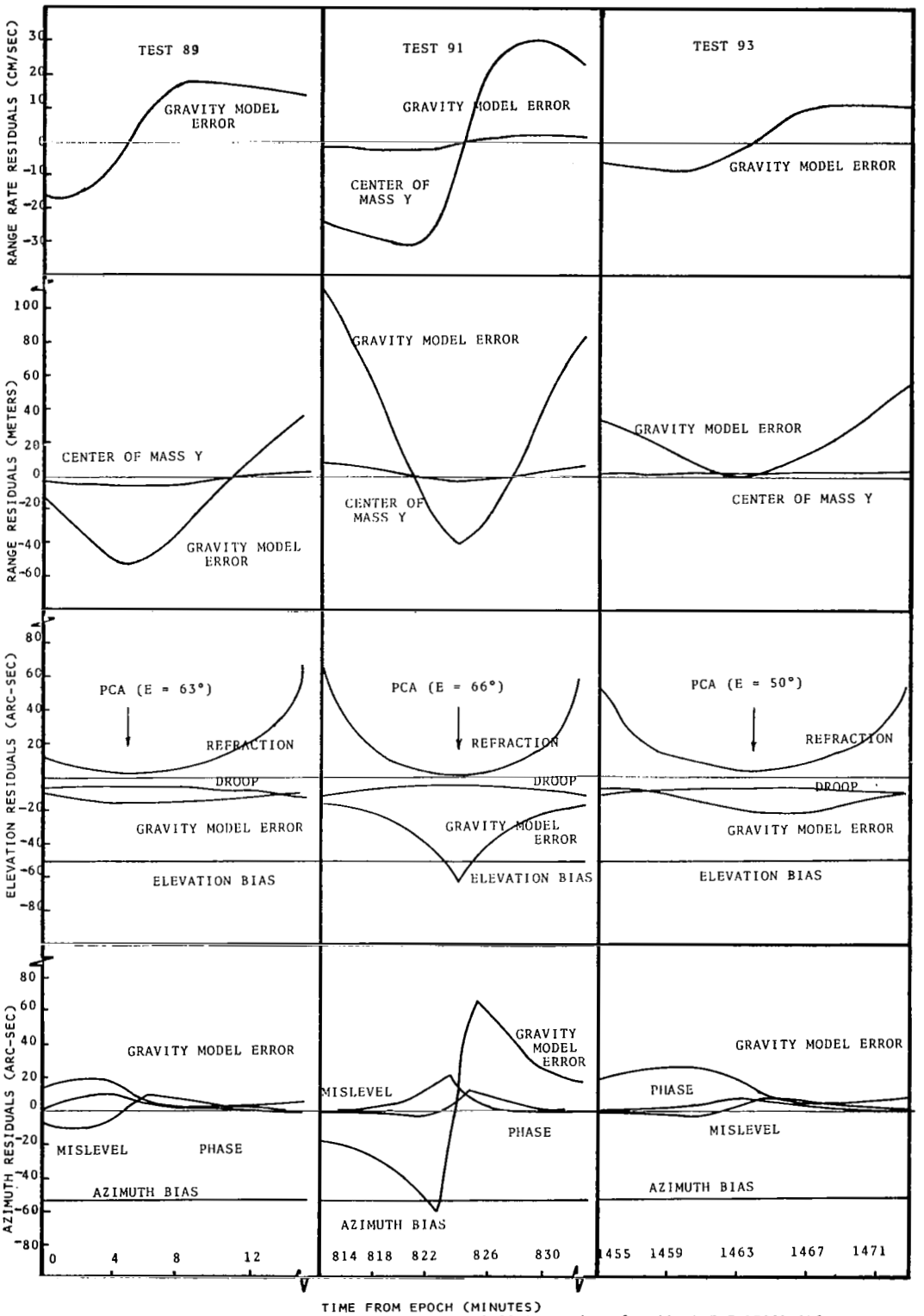

FIGURE 10 MAJOR UNMODELED ERROR EFFECTS ON WALLOPS ISLAND AN/FPQ-6 MEASUREMENT RESIDUALS ONE DAY LONG ARC SOLUTION

This effect is consistent with the azimuth and elevation bias effects on the epoch elements as shown in Table 7. That is, these measurements have an essentially negligible effect on the orbit. (As a corollary, this means that the azimuth and elevation measurements had little effect on the solution. This is the case because of their low weights in the solution and the fact that the multiple pass solution is possible using range and/or range rate data alone.) Since the orbit does not shift to reduce the azimuth or elevation biases, the total bias remains in the residuals.

It will be noted that some of the radar error model terms, elevation droop and mislevel, can show up in the azimuth and elevation residuals. As was the case with biases, we again have the effect on the measurement propagated directly into the residual with practically no effect upon the orbit.

4.2.3 Characteristics of Single Station Long Arc Solution

From the tables and graphs shown above, several distinguishing characteristics may be deduced for the long arc solution as follows:

a. The noise only variance for the orbit is much lower than the single pass solution. It would appear that the variation during a revolution would have a minimum for each tracking pass of significantly geometry, although not all minima would be expected to occur during tracking periods.

b. The orbit is determined almost completely (with the weights used) by the range and range rate data.

c. Errors in the azimuth and elevation measurements will be seen in their residuals in a form distorted only by a geopotential coefficient error and the (possible) presence of several different error sources.

d. By far the most significant source of orbital error consists of errors in the geopotential coefficients.

e. Large trended range and range rate residuals can arise in multi-pass solutions from geopotential coefficient errors.

SECTION 5.0
UNMODELED ERROR EFFECTS ON SELECTED MULTIPLE STATION SOLUTIONS

5.1 SHORT ARC MULTI-STATION

The pass selected for the unmodeled error analysis was identical to the high elevation, single station solution presented in Section 4.0 (collocation test 89). The following AN/FPQ-6 radars were utilized for the multiple station solution: Patrick AFB, Wallops Island, Bermuda and Antigua. The pass configuration in respect to each station has fairly well represented a high elevation geometry from Wallops and Bermuda, and a low elevation geometry from Antigua and Patrick. The short arc case was investigated to determine the effects of unmodeled errors in the measurement residuals and orbit prediction accuracy attainable from multiple stations.

For multiple station data reduction analysis, it is reasonable to expect any systematic errors to be uncorrelated between the stations. This assumption is similarly applied to multiple station error analysis studies. Thus, the results obtained from each station are completely independent of the other stations. Standard measurements included range, azimuth and elevation data from all stations with the addition of rate data from the Wallops radar.

5.1.1 Orbit Accuracy

The multiple station error estimates in the HCL coordinate system are presented in Table 8. A comparison with the single station solution shows a decrease due to the effects of the following unmodeled errors on the orbit: range-rate bias, azimuth and elevation bias, refraction and geopotential errors. The local survey, center of mass coordinates, and range bias were relatively unaffected. The largest improvement over the single station solution was the angle bias and refraction errors. In addition, the total measurement noise on the orbit is less than 3.0 meters, an improvement over the single station by a factor of ten for the same arc.

Figure 11 presents the total rss orbit accuracy for one revolution past epoch. During the data span the orbit accuracy due to noise is 2.1 meters and due to noise plus unmodeled errors is 42 meters; if no measurements were available on the next consecutive tracking period the orbit accuracies would be 44 and 500 meters, respectively. The lack of a deep variance minimum on the subsequent revolution for multiple radars is due to the relatively poor geometry between the four stations (see Figure 2). From this analysis, it is clear that the multiple radar solution is about ten times better than the single radar solution at most time points.

5.1.2 Residuals

Figure 12 illustrates the major unmodeled error effects on the measurement residuals. It is interesting to investigate whether the reduction in the orbit error

TABLE 8

MULTI-STATION SHORT ARC SOLUTION (TEST 89)

ESTIMATED HCL ERROR ON EPOCH ELEMENTS DUE TO UNMODELED PARAMETERS

DELTA H (METERS)	DELTA C (METERS)	DELTA L (METERS)	DELTA HDOT (CM/SEC)	DELTA CDOT (CM/SEC)	DELTA LDOT (CM/SEC)	UNADJUSTED PARAMETER
1.51	2.41	1.64	0.69	0.76	0.26	NOISE
0.84	1.30	6.04	-1.62	0.03	-0.91	WAL R BIAS
-3.06	1.20	-5.60	1.82	0.10	0.60	ANT R BIAS
-4.02	-4.23	-1.83	0.33	-1.21	-0.25	PAT R BIAS
-0.06	3.46	0.74	0.11	0.92	-0.02	BER R BIAS
0.43	3.29	-1.10	0.09	-1.52	-0.13	WAL A BIAS
-0.75	-1.41	-0.94	0.30	0.21	0.11	ANT A BIAS
2.00	3.16	3.17	-1.29	-1.57	-0.52	PAT A BIAS
-0.46	0.27	-1.36	0.33	-0.43	0.06	BER A BIAS
1.02	0.20	1.32	-1.05	-0.77	-0.18	WAL E BIAS
-0.32	-0.82	0.22	-0.04	0.11	-0.01	ANT E BIAS
1.23	1.47	1.51	-0.81	-0.42	-0.15	PAT E BIAS
-0.01	-0.91	0.53	-0.41	-0.20	-0.06	BER E BIAS
-4.26	1.85	-7.66	2.53	0.06	0.82	ANTIGA X
3.51	-0.95	6.80	-2.11	-0.30	-0.75	ANTIGA Y
2.28	-1.24	3.84	-1.34	0.10	-0.40	ANTIGA Z
0.02	5.31	0.94	0.08	1.19	0.00	BERMDA X
0.94	6.36	1.99	-0.63	-3.28	-0.43	BERMDA Y
-0.31	-5.61	-1.15	0.15	0.10	0.10	BERMDA Z

TABLE 8 (cont.)

DELTA H (METERS)	DELTA C (METERS)	DELTA L (METERS)	DELTA HDOT (CM/SEC)	DELTA CDOT (CM/SEC)	DELTA LDOT (CM/SEC)	UNADJUSTED PARAMETER
-0.88	-1.89	-2.08	0.78	0.66	0.14	WAL RR BIAS
-0.39	-0.39	-1.35	0.37	0.21	0.26	WALLPS REF
0.53	0.12	0.82	-0.23	-0.06	-0.09	ANTIGA REF
-0.49	-0.71	-0.70	0.45	0.58	0.19	PATRIK REF
-0.25	-0.88	-0.53	0.25	-0.12	0.06	BERMDA REF
0.57	-0.99	-0.57	-0.06	0.41	-0.08	WALLPS TIM
-1.37	0.44	-2.59	0.82	0.09	0.28	ANTIGA TIM
0.95	2.07	-0.00	-0.61	-1.48	-0.32	PATRIK TIM
-0.25	-1.27	-0.46	0.18	0.97	0.12	BERMDA TIM
1.68	0.06	3.08	-1.55	0.35	-0.51	WALLPS X
-1.42	3.77	3.37	-0.46	-1.42	0.12	WALLPS Y
-2.50	-2.60	-7.48	3.39	0.41	0.73	WALLPS Z
3.07	5.12	0.89	-1.10	-1.93	-0.45	PATRIK X
-2.57	-5.99	0.15	1.87	4.71	1.01	PATRIK Y
8.74	11.65	4.19	-1.84	-0.52	-0.32	PATRIK Z
-4.64	-17.35	7.06	0.03	-0.58	0.30	C.O.M. X
18.26	-6.93	-4.44	-0.34	0.04	-0.62	C.O.M. Y
-7.72	-5.43	-17.74	0.46	-0.11	-0.28	C.O.M. Z
1.08	1.42	1.43	-1.07	-1.12	-0.63	NWL-SAO GRAV
-0.10	-0.01	-0.13	0.12	-0.01	0.07	GRAV COEF
24.42	27.97	26.74	6.94	7.44	2.59	TOTAL ERROR

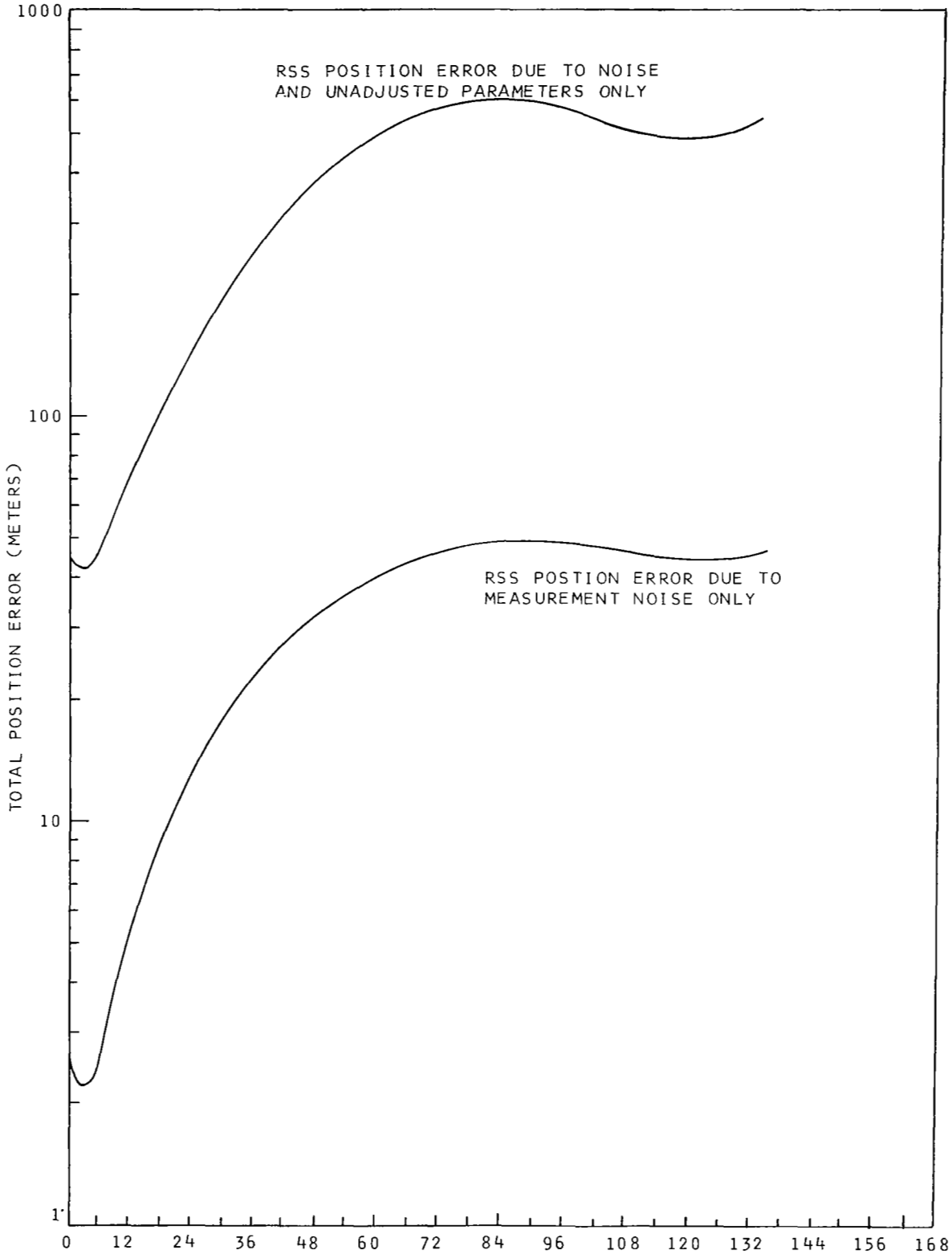

FIGURE 11 TOTAL ORBIT ACCURACY FOR MULTIPLE STATION SHORT ARC

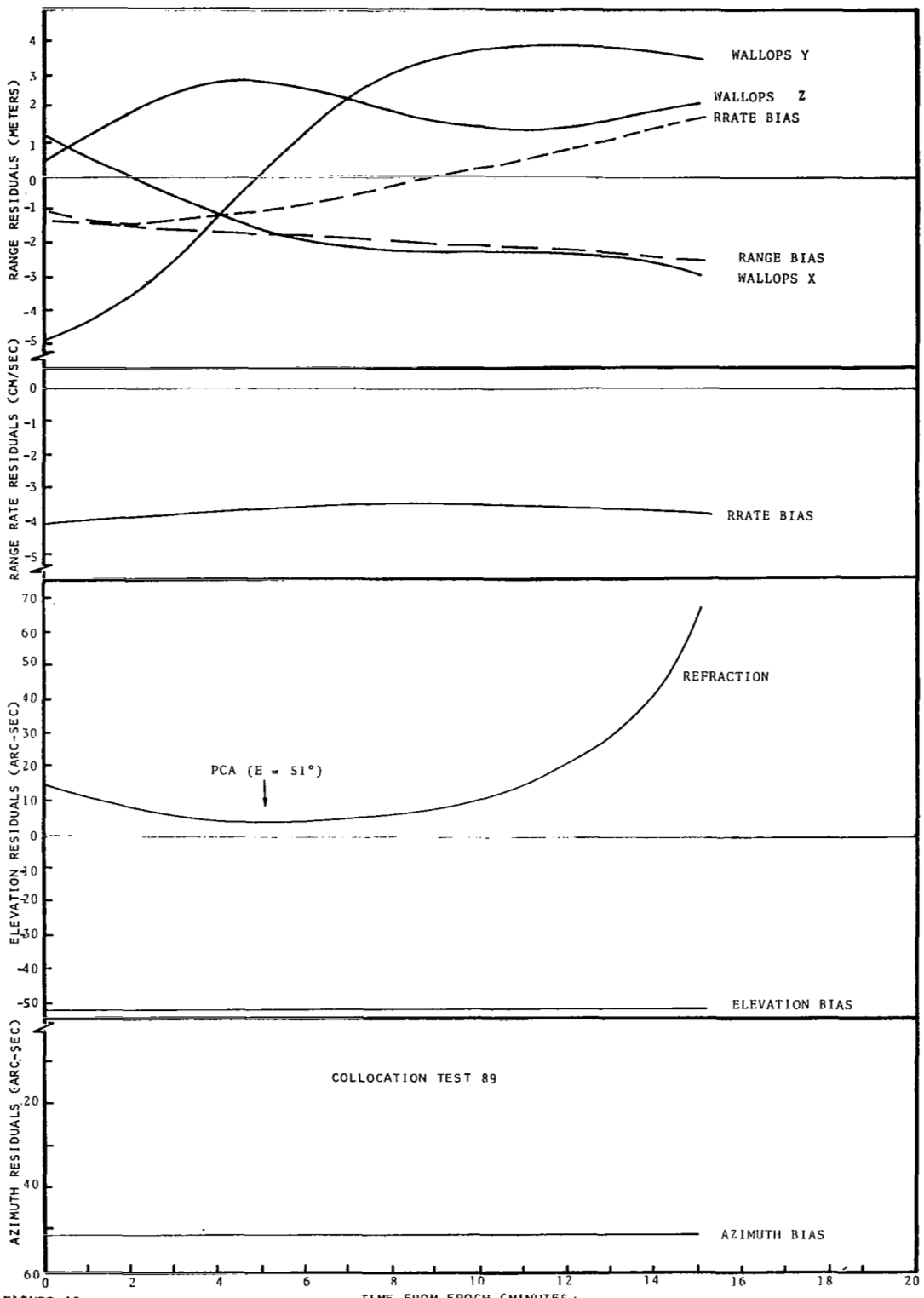

FIGURE 12 WALLOPS MAJOR UNMODELED ERROR EFFECTS ON WALLOPS ISLAND AN/FPQ-6 MEASUREMENT RESIDUALS FOR TYPICAL MULTIPLE STATION SHORT ARC

for the multiple station solution was transformed into the measurement residuals. Figure 12 clearly shows that the azimuth and elevation bias errors were almost totally absorbed by the residuals. This was not the case for the single station solution where the angle bias errors were almost totally absorbed by the orbit. Thus, for multiple radar short arc solutions, the orbit does not act as a filter and absorb systematic errors in the tracking system as was the case for single radar short arcs; in the former case, the geometry between the stations helps to improve the overall minimum variance solution and distributes the systematic errors appropriately.

5.1.3 Characteristics of Short Arc Solution

From the analysis conducted on a typical short arc multi-station solution, the following characteristics were observed:

A. Angle biases are completely absorbed by the measurement residuals.

B. Geopotential, timing and hardware errors were relatively insignificant.

C. Refraction errors are nearly all absorbed by the elevation residuals.

D. The multiple radar solution is approximately ten times better than the single radar solution.

5.2 LONG ARC MULTIPLE STATION

We now consider the reduced data characteristics for tracking by the same station configuration discussed in the previous section, but with tracking over a period of 2 days as indicated in Table [9]. These passes correspond to collocation test numbers 84, 88, and 91. Reference to Figure 2 shows that the pass geometry was similar on the first and third pass, but quite different (i.e., the opposite side of the orbit) on the second pass.

The unmodeled error set we consider to be the same as for the short arc case, with all measurement biases the same for the duration of the complete tracking period. This is, of course, an approximation since the correlation of radar biases from one pass to the next will be less than perfect. In terms of total orbital error computation, however, the assumption made is the pessimistic one and is consistent with the general approach in this report of considering upper limits for various error sources.

5.2.1 Orbital Accuracy

The standard deviations of the orbital elements due to measurement noise alone are shown in the first row of Table 10. Again we note the noise only sigmas to be considerably reduced from those for the single pass solution. A breakdown of the unmodeled error effects on the epoch elements is also shown in Table 10. The last row in the table gives the total standard deviations including both modeled and unmodeled effects. As was

Station	PASS 1 Tracking Time (minutes from epoch)	PASS 1 Max. El. (degrees)	PASS 2 Tracking Time (minutes from epoch)	PASS 2 Max. El. (degrees)	PASS 3 Tracking Time (minutes from epoch)	PASS 3 Max. El. (degrees)
Wallops	0.0 -14.25	26.6	1879.75-1897.25	33.5	2806.5 -2825.5	65.9
Antigua			1878. -1889.25	31.5	2814.75-2825.	11.2
Patrick AFB	1.75-16.75	21.1	1880.5 -1893.25	15.4	2810. -2828.75	63.7
Bermuda	0.5 -10.25	10.0	1878. -1894.75	46.4	2807.75-2824.5	30.4

TABLE 9
TRACKING ON MULTI-STATION LONG ARC

TABLE 10

MULTIPLE STATION TWO DAY LONG ARC SOLUTION

ESTIMATED HCL ERROR ON EPOCH ELEMENTS DUE TO UNMODELED PARAMETERS

DELTA H (METERS)	DELTA C (METERS)	DELTA L (METERS)	DELTA HDOT (CM/SEC)	DELTA CDOT (CM/SEC)	DELTA LDOT (CM/SEC)	UNADJUSTED PARAMETER
0.37	0.63	1.04	0.09	0.09	0.03	NOISE
-0.24	-3.25	-2.31	0.01	0.36	0.02	WAL R BIAS
0.26	-1.68	0.01	0.15	-0.06	-0.02	ANT R BIAS
-0.35	-2.80	-0.84	-0.09	0.27	0.03	PAT R BIAS
0.66	-4.15	0.07	0.12	0.03	-0.06	BER R BIAS
0.06	0.04	1.08	-0.06	-0.05	-0.01	WAL A BIAS
-0.07	-0.03	-0.27	-0.03	0.06	0.01	ANT A BIAS
-0.20	0.34	0.74	-0.08	-0.01	0.02	PAT A BIAS
0.06	-0.09	0.49	-0.04	0.00	-0.01	BER A BIAS
-0.49	0.83	-0.06	-0.06	0.02	0.04	WAL E BIAS
0.01	0.11	0.20	0.00	-0.03	-0.00	ANT E BIAS
-0.67	0.78	-0.49	-0.07	0.09	0.05	PAT E BIAS
-0.22	0.53	0.20	-0.02	-0.03	0.02	BER E BIAS
0.19	-1.32	0.31	-0.03	-0.22	-0.02	ANTIGA X
0.03	1.60	0.13	-0.23	0.10	-0.01	ANTIGA Y
-0.19	0.82	-0.00	-0.09	-0.01	0.02	ANTIGA Z
-0.15	-2.35	-0.38	0.03	-0.22	0.01	BERMDA X
0.56	2.94	-0.58	-0.22	0.18	-0.05	BERMDA Y
-0.51	2.66	0.03	-0.11	-0.05	0.04	BERMDA Z
-0.08	0.03	-2.24	0.16	0.02	0.01	WAL RR BIAS

TABLE 10 (CONT.)

DELTA H (METERS)	DELTA C (METERS)	DELTA L (METERS)	DELTA HDOT (CM/SEC)	DELTA CDOT (CM/SEC)	DELTA LDOT (CM/SEC)	UNADJUSTED PARAMETER
0.02	0.37	0.43	-0.02	-0.04	-0.00	WALLPS REF
0.02	0.30	0.02	-0.02	0.02	0.00	ANTIGA REF
0.11	0.44	0.11	0.02	-0.06	-0.01	PATRIK REF
0.05	0.60	-0.03	0.00	-0.01	-0.00	BERMDA REF
-0.19	0.01	-2.21	0.11	0.07	0.02	WALLPS TIM
-0.03	0.02	0.08	0.04	-0.03	0.00	ANTIGA TIM
0.57	-0.58	-1.03	0.14	-0.03	-0.05	PATRIK TIM
-0.32	0.48	-0.42	0.04	-0.03	0.03	BERMDA TIM
-0.82	-0.15	-4.59	0.20	-0.12	0.08	WALLPS X
1.84	0.58	-2.58	0.10	0.04	-0.17	WALLPS Y
1.20	1.83	2.30	0.15	-0.44	-0.11	WALLPS Z
0.66	-1.00	0.27	0.15	-0.55	-0.06	PATRIK X
2.25	0.70	-1.80	0.38	-0.33	-0.20	PATRIK Y
1.08	0.93	1.53	0.17	-0.28	-0.10	PATRIK Z
1.14	7.27	5.81	-0.73	2.48	-0.11	C.O.M. X
-2.06	8.50	13.67	-0.09	-0.59	0.10	C.O.M. Y
-9.72	-16.64	3.64	-0.20	0.90	0.88	C.O.M. Z
66.35	-42.27	25.69	-12.51	14.70	-4.90	NWL-SAO GRAV
2.29	-3.55	-1.35	-0.00	0.27	0.30	GRAV COEF
67.25	47.70	30.91	12.56	14.99	5.00	TOTAL ERROR

the case with the single station long arc solution, the dominant error source is geopotential coefficient errors. The only other really significant errors are due to center of mass errors. The overall orbital accuracy, both total and noise only, is shown in Figure 13 as a function of time for slightly more than one revolution. In contrast to the single station solution, the noise only variance has but a single cycle during a revolution, in spite of the fact that the orbit determination includes data on both sides of the orbit. The most likely explanation for this behavior is that the more spread out tracking configuration observes a sufficiently large portion of the orbit and from sufficiently different aspect angles that sharp variations in the orbital accuracy during a revolution are precluded. It will be noted that a minimum orbital error occurs prior to rather than during the first pass, no doubt an influence of the other two passes.

The time behavior of the total orbital accuracy is, of course, not fully depicted by one revolution. However, the basic pattern of behavior is quite similar to that for the single station solution. The orbital error is due almost entirely to geopotential coefficient errors, each component of which is a near sinusoid with the period of the orbit. Converting the components into an rss error effectively doubles the frequency. The time varying phases produce interference patterns which should vary somewhat irregularly during the day, but should repeat themselves after a day.

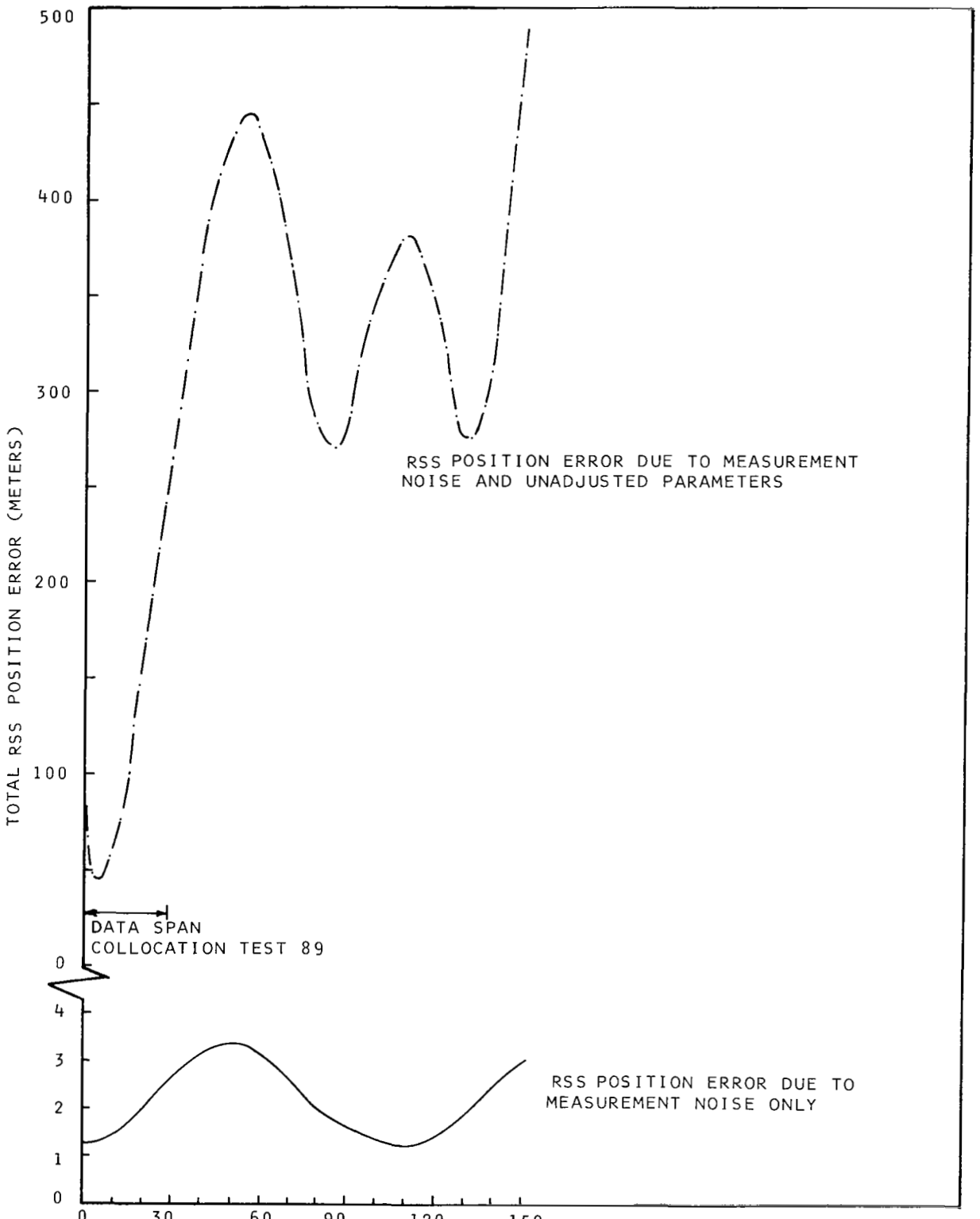

FIGURE 13 TOTAL ORBIT ACCURACY ON MULTIPLE STATION LONG ARC SOLUTION FOR UNADJUSTED PARAMETERS

5.2.2 Residuals

Residual computations for the most significant effects on the Wallops radar measurements for all three passes are shown in Figure 14. As expected, the geopotential coefficient errors produce one of the dominant effects. But various other errors, particularly biases, are quite evident. For the angles, only the biases and refraction produce significant effects. Center of mass errors, although noticeable in the orbital elements, cannot be seen in the residuals.

5.2.3 Characteristics of Long Arc Multi-Station Solutions

The fact that biases in measurements look like biases in the residuals indicates that the orbit has a limited ability to absorb systematic errors from the number of stations and measurements used in the solution considered here. The same trend was evident in both the single station long arc and the multi-station short arc.

Geopotential coefficient errors lead to trended effects in all residuals, and are the dominant contributors to range residuals only. For the other measurements, the bias errors are comparable to or much greater than the geopotential error effects.

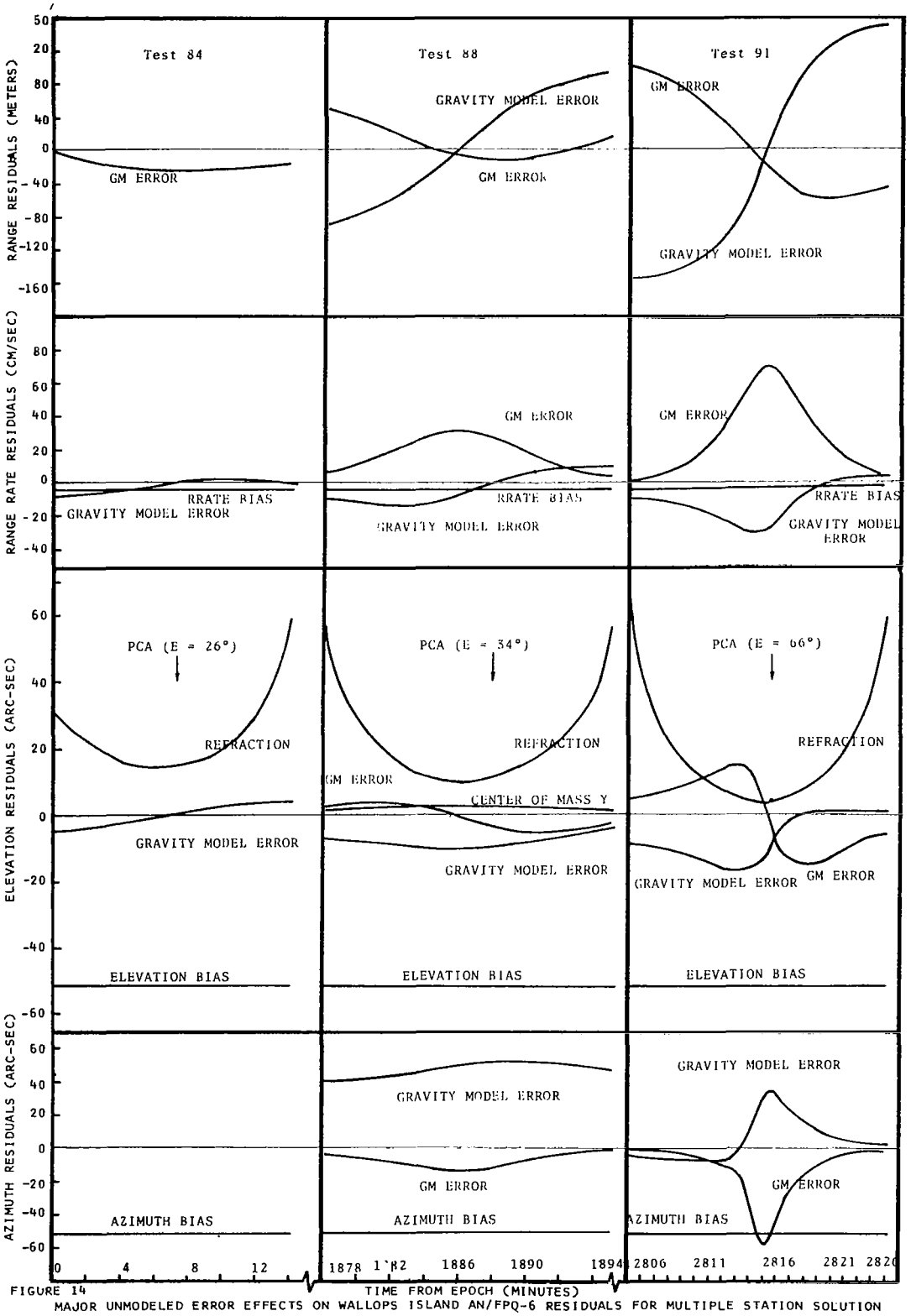

FIGURE 14
MAJOR UNMODELED ERROR EFFECTS ON WALLOPS ISLAND AN/FPQ-6 RESIDUALS FOR MULTIPLE STATION SOLUTION

SECTION 6.0
PROBLEMS IN ERROR MODEL RECOVERY

6.1 GENERAL

In Sections 3,4, and 5, we have acknowledged the existence of certain systematic errors in the FPQ-6 radar measurements and we have found that when such errors are ignored, significant orbital errors result. Since it has been implicitly assumed that error model expressions exist for such systematic effects (with the exception of geopotential coefficient errors), we now wish to consider the capabilities of the data reduction process for recovering some of the error model coefficients. In this section, we will examine the error model recovery capabilities from two widely different types of arcs: a single station, single pass short arc, and a 48 hour arc with 3 passes over a network of 4 tracking stations. We might expect different answers because of the different characteristics of the two arcs.

6.2 SHORT ARC RECOVERY

A range, azimuth and elevation bias recovery was performed on the Wallops single pass solution for collocation test 89. The minimum variance solution for this case now solves for both the epoch orbital elements and the three measurement biases simultaneously.

6.2.1 Orbit Accuarcy

The error estimates for the orbital elements in the HCL coordinate system are presented in Table 11, including the effects of each unadjusted parameter. Comparing these

TABLE 11

SINGLE STATION SHORT ARC WITH BIAS RECOVERY (TEST 89)

ESTIMATED HCL ERROR ON EPOCH ELEMENTS DUE TO UNMODELED PARAMETERS

DELTA H (METERS)	DELTA C (METERS)	DELTA L (METERS)	DELTA HDOT (CM/SEC)	DELTA CDOT (CM/SEC)	DELTA LDOT (CM/SEC)	UNADJUSTED PARAMETER
14.78	433.65	130.87	17.21	142.02	7.17	NOISE
-15.48	-77.73	1.26	4.49	25.68	3.23	R RTE BIAS
-0.38	17.25	-4.88	-0.09	-6.29	-0.73	NWL-SAO GRAV
-0.29	-1.34	0.10	0.14	0.40	0.11	GRAV COEF
-9.04	-323.25	75.47	-8.44	94.69	5.88	REFRACTION
-3.15	-6.26	5.60	-0.21	-4.28	0.06	C.O.M. X
16.66	-14.62	-4.10	0.04	2.73	-0.30	C.O.M. Y
-11.05	-15.91	-18.26	1.41	3.27	0.24	C.O.M. Z
30.81	547.16	152.41	19.74	172.84	9.85	TOTAL ERROR

results with those for the short arc unadjusted solution, we see that not only are the noise only sigmas much larger, but the individual unmodeled error effects are considerably larger also. (not shown are the correlation coefficients between the orbital elements, which are also larger for the adjusted parameter case.) In particular, the measurement noise effects on the epoch elements for the bias recovery solution are more than an order of magnitude greater than they are for the unadjusted parameter solution. All these factors indicate that an attempt to recover measurement biases on a short arc pass leads to a near singular solution.

Table 12 presents the results of the instrumentation bias adjustment for a single radar short arc solution. These results demonstrate the futility of short arc bias recovery solutions using a single radar. The simulation results indicate that if data is utilized from only a single pass, the potential for recovery of instrumentation biases is quite good in elevation, but poor in azimuth, and extremely poor in range. Thus, had we attempted to adjust only the bias in elevation, we may have obtained a better orbital solution and a fairly good elevation bias adjustment. It is apparent that as more parameters are adjusted, the solution becomes more sensitive to the effects of unadjusted errors.

The total orbital accuracy during the data period is presented in Figure 15 and should be compared with Figure 3 which shows the rss orbital accuracy for the same solution except with no parameter adjustments. The orbital accuracy for the former solution is also shown for one revolution past epoch. During this error propagation, it is clear that the measurement noise in the orbit is larger than in the unadjusted short arc solution by at least a

TABLE 12

SINGLE STATION SHORT ARC WITH BIAS RECOVERY (TEST 89)

STANDARD DEVIATIONS FOR ADJUSTED PARAMETERS

PARAMETER	SIGMA AFTER ADJUSTMENT	RATIO TO A PRIORI	SIGMA INCL. UNADJ. PAR.	A PRIORI SIGMA	MAXIMUM UNMOD. PAR.	MAGNITUDE
RANGE BIAS	4.84 meters	0.9683	5.63 meters	5.0 meters	REFRACTION	2.8 meters
AZMTH BIAS	40.3 arc-sec	0.8298	51.3 arc-sec	51.5 arc-sec	REFRACTION	26.8 arc-sec
ELEVN BIAS	2.45 arc-sec	0.0476	16.6 arc-sec	51.5 arc-sec	REFRACTION	16.6 arc-sec

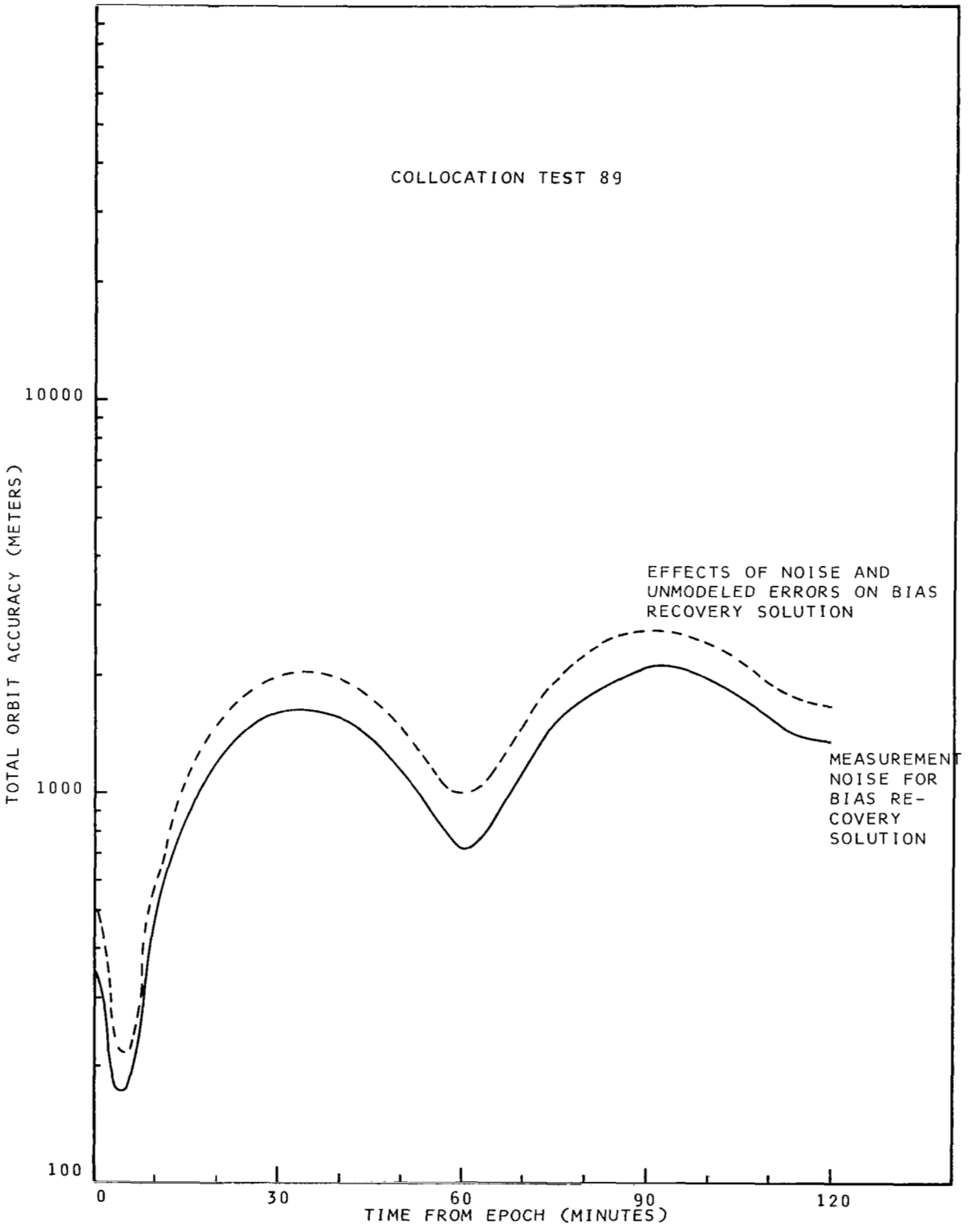

FIGURE 15 TOTAL RSS ORBIT ACCURACY FOR SINGLE RADAR SHORT ARC BIAS RECOVERY

factor of six for most time points, and that the effects of the unmodeled errors contribute a maximum of approximately 300 meters to the orbit uncertainty as opposed to 1000 meters for the unadjusted solution.

6.2.2 Characteristics of Short Arc Bias Recovery

From the analysis conducted on the short arc single radar bias recovery, the following characteristics have been observed:

a. Bias recovery may be quite good in elevation but is generally poor in azimuth and range.

b. As more parameters are adjusted, the solution becomes more singular and more sensitive to small errors in unadjusted parameters.

6.3 MULTIPLE STATION LONG ARC SOLUTION WITH BIAS ADJUSTMENTS

To demonstrate the error model recovery capabilities of multi-station multi-revolution arcs, the same tracking configuration discussed in Section 5.2 was re-run in ORAN with the same set of error model terms, but with certain of the error model terms switched to the adjusted category. These included range, azimuth, and elevation biases for all radars and the positions of the Antigua and Bermuda radars. The same a priori information was used for the adjusted parameters as had been used for the magnitudes of the expected error in the parameters when they were considered to be unadjusted.

TABLE 13

MULTI-STATION LONG ARC ADJUSTMENT SOLUTION (TESTS 84,88,91)

ESTIMATED HCL ERROR ON EPOCH ELEMENTS DUE TO UNMODELED PARAMETERS

DELTA H (METERS)	DELTA C (METERS)	DELTA L (METERS)	DELTA HDOT (CM/SEC)	DELTA CDOT (CM/SEC)	DELTA LDOT (CM/SEC)	UNADJUSTED PARAMETER
0.39	1.44	1.10	0.10	0.11	0.04	NOISE
-0.11	-0.89	-2.48	0.18	0.03	0.01	WAL RR BIAS
-0.25	-0.06	-0.05	-0.04	0.04	0.02	WALLPS REF
0.06	0.03	0.17	0.02	-0.03	-0.01	ANTIGA REF
-0.28	0.58	-0.28	-0.05	0.04	0.02	PATRIK REF
0.03	0.27	0.20	0.01	-0.04	-0.00	BERMDA REF
-0.19	-1.47	-2.58	0.13	0.09	0.02	WALLPS TIM
-0.04	0.63	0.23	0.02	-0.04	0.00	ANTIGA TIM
0.65	-1.34	-1.19	0.14	-0.02	-0.06	PATRIK TIM
-0.38	2.08	-0.02	0.03	-0.05	0.03	BERMDA TIM
-0.87	-4.45	-5.15	0.24	--0.25	0.08	WALLPS X
2.31	2.72	-3.31	-0.15	0.23	-0.21	WALLPS Y
1.08	0.52	0.83	0.15	-0.20	-0.10	WALLPS Z
0.78	-0.72	0.78	0.12	-0.88	-0.07	PATRIK X
2.37	2.53	-1.51	0.15	-0.27	-0.21	PATRIK Y
0.91	-1.85	0.83	0.16	-0.06	-0.08	PATRIK Z
0.57	11.70	6.65	-0.83	2.36	-0.06	C.O.M. X
-1.57	-5.34	10.42	0.38	-0.03	0.15	C.O.M. Y
-10.03	-7.76	6.07	-0.33	0.41	0.81	C.O.M. Z
58.07	-80.46	20.86	-12.21	13.83	-5.06	NWL-SAO GRAV
2.16	0.47	-0.14	-0.10	0.06	0.29	GRAV COEF
68.97	82.15	26.12	12.26	14.07	5.16	TOTAL ERROR

6.3.1 Orbit Accuracy

The accuracy of the recovered orbital elements, along with the various contributions to the total error, are shown in Table 13. A comparison with Table 10, which shows the comparable quantities when only the orbital elements are solved for, shows that:

a. The "noise" contribution to the total uncertainty is considerably larger, although still a minor contributor to the total orbital error.

b. The effects of the unmodeled errors have, in general, increased.

c. The most significant unadjusted parameters are still the same, with the gravity model difference responsible for the largest error, and the only other relatively significant parameters being center of mass errors.

d. The overall accuracy of the epoch elements has not significantly changed, being slightly smaller for the adjusted parameter case.

The time propagation of the overall orbital error is shown in Figure 16 for slightly more than one revolution after epoch. This period includes the first tracking period. As was indicated by the orbital elements, the noise only solution shows a much larger uncertainty when parameters other than the epoch elements are solved for, but the overall uncertainty is not significantly different when the effects of the unadjusted parameters are included.

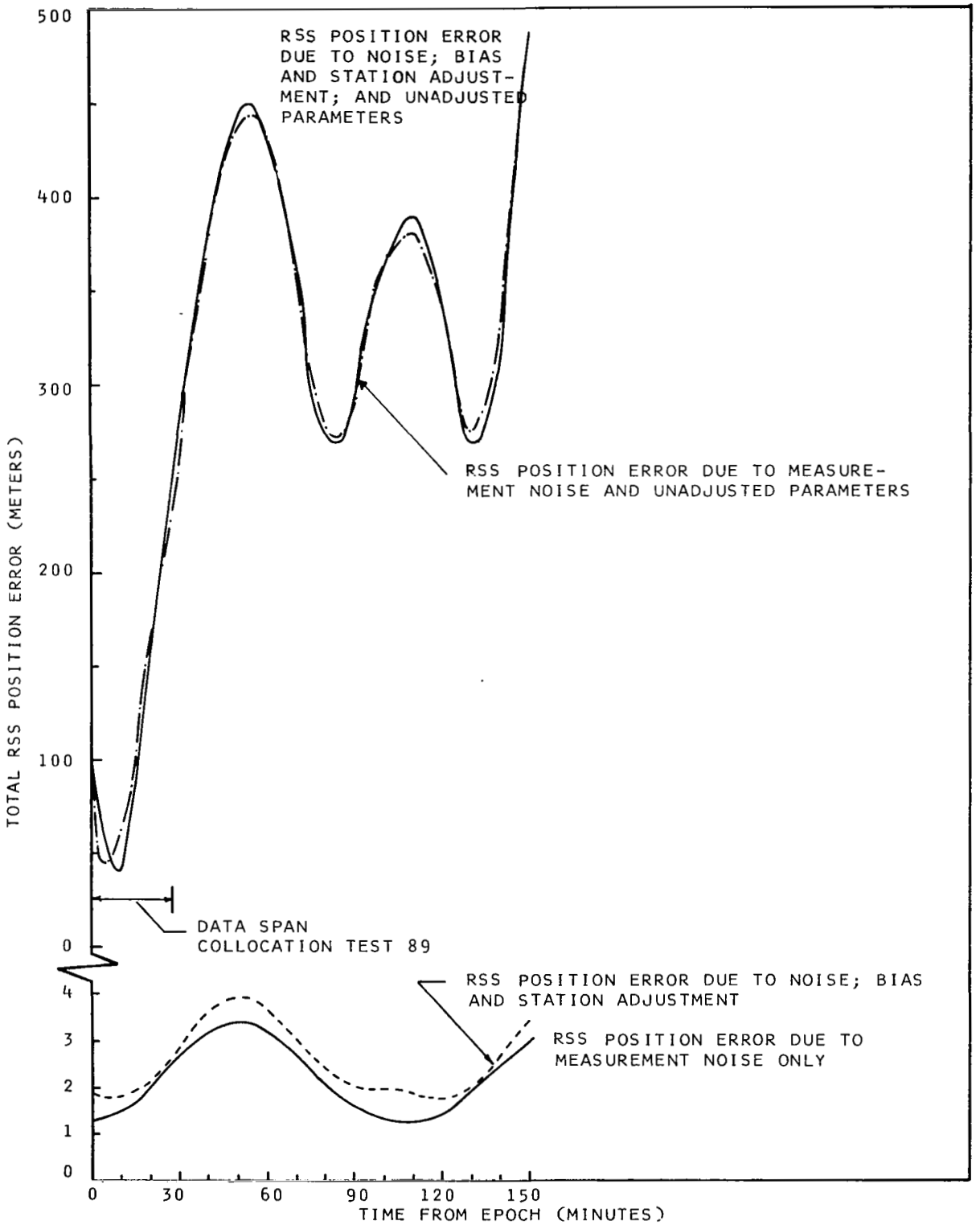

FIGURE 16 TOTAL ORBIT ACCURACY ON MULTIPLE STATION LONG ARC SOLUTION FOR ADJUSTED VS UNADJUSTED PARAMETERS

6.3.2 Adjusted Parameter Accuracy

The standard deviations of the adjusted biases and station positions are shown in Table 14. Three sets of sigmas are shown: the a priori, the adjusted sigmas including noise contributions only, and the adjusted sigmas including all unmodeled error effects. In addition, the most significant unadjusted parameters and their effects are shown.

Several features of the entries in Table 14 are immediately evident:

a. Considering the noise only solution, there was a large reduction in the a priori sigma for all parameters. The poorest recovery was in the Bermuda height, for which the adjusted sigma was 59% of the a priori.

b. With one exception, the total uncertainties after adjustment of the range biases and station positions were greater than the a priori uncertainties. The one exception is the Y, or latitude, coordinate of Bermuda. It will be noted that in this case, the largest contributor to the total uncertainty is the latitude of the Wallops radar. This indicates that, as might be expected on a geometrical basis, the error in the adjusted latitude of Bermuda would be essentially the same as the error in the Wallops latitude.

c. Even including the unmodeled error effects, the adjustment of the elevation biases from all stations is good (reduction of the a

TABLE 14

MULTI-STATION LONG ARC BIAS RECOVERY UNCERTAINTIES

PARAMETER	STANDARD DEVIATIONS			MOST SIGNIFICANT UNADJUSTED PARAMETER	
	A Priori	Adjusted			
		Noise Only	Total	Name	Effect
Bermuda R Bias	5.000 m	1.111 m	22.190 m	NWL-SAO Grav	21.633 m
Patrick R Bias	5.000 m	0.574 m	11.266 m	NWL-SAO Grav	7.777 m
Wallops R Bias	5.000 m	0.571 m	12.245 m	NWL-SAO Grav	9.175 m
Antigua R Bias	5.000 m	2.388 m	17.520 m	NWL-SAO Grav	17.964 m
Wallops A Bias	0.250 mr	0.005 mr	0.007 mr	NWL-SAO Grav	0.004 mr
Antigua A Bias	0.250 mr	0.008 mr	0.023 mr	NWL-SAO Grav	0.021 mr
Patrick A Bias	0.250 mr	0.005 mr	0.010 mr	NWL-SAO Grav	0.008 mr
Bermuda A Bias	0.250 mr	0.005 mr	0.010 mr	NWL-SAO Grav	0.008 mr
Wallops E Bias	0.250 mr	0.005 mr	0.110 mr	Wallops Refr	0.104 mr
Antigua E Bias	0.250 mr	0.008 mr	0.157 mr	Antigua Refr	0.154 mr
Patrick E Bias	0.250 mr	0.005 mr	0.133 mr	Patrick Refr	0.131 mr
Bermuda E Bias	0.250 mr	0.006 mr	0.135 mr	Bermuda Refr	0.132 mr
Antigua X	10.000 m	1.558 m	56.723 m	NWL-SAO Grav	56.002 m
Antigua Y	10.000 m	1.861 m	13.987 m	NWL-SAO Grav	8.445 m
Antigua Z	10.000 m	5.930 m	25.630 m	NWL-SAO Grav	17.751 m
Bermuda X	10.000 m	0.880 m	23.900 m	NWL-SAO Grav	22.474 m
Bermuda Y	10.000 m	0.910 m	8.706 m	Wallops Y	6.266 m
Bermuda Z	10.000 m	2.289 m	35.775 m	NWL-SAO Grav	26.577 m

Units: m - meters
mr - milliradians

priori sigma by about a factor of two, even with the use of pessimistic values for the uncertainties in the unadjusted parameters) and the recovery of the azimuth biases is excellent (reduction of the a priori sigma by at least a factor of ten).

d. The elevation angle biases are corrupted much more by refraction than by geopotential coefficient errors.

e. In general, errors in the geopotential model and correlations between different error model terms constitute the largest deterrents to radar calibration using long arc orbital solutions.

SECTION 7.0
DATA ANALYSIS

7.1 SHORT ARC COMPARISONS

To demonstrate the usage of ORAN for data analysis, an attempt was made to determine those error model parameters which can satisfactorily account in particular cases for the systematic part of actual AN/FPQ-6 tracking residuals. Two actual pass sets of data taken by the Wallops AN/FPQ-6 radar on GEOS II were investigated. Collocation tests 84 and 87 were selected for study representing, respectively, two low elevation pass configurations. The actual NONAME data reduction range residuals were randomly distributed but the angle residuals were systematically trended. Figures 17 through 22 present the NONAME residuals for both tests with points plotted every 15 seconds apart. These graphs adequately represent the gross features of the actual FPQ-6 tracking residuals.

ORAN simulations were made using the same measurement weights as were used in the NONAME data reduction (σ_R = 2 meters and $\sigma_{A,E}$ = 50 arc - sec), and unmodeled parameter effects were computed on the resulting range, azimuth and elevation residuals. The object of this investigation was to determine the effects of independent instrumentation errors on the radar-orbit geometry and the subsequent radar residuals. The unmodeled errors and their magnitudes were selected from Table 3 and represent the best current knowledge of the error sources.

The unmodeled error effects on the measurement residuals computed from the ORAN simulations are presented in Figures 17, 18 and 19 for test 87 and Figures 20, 21 and 22 for test 84. Only the most significant unmodeled

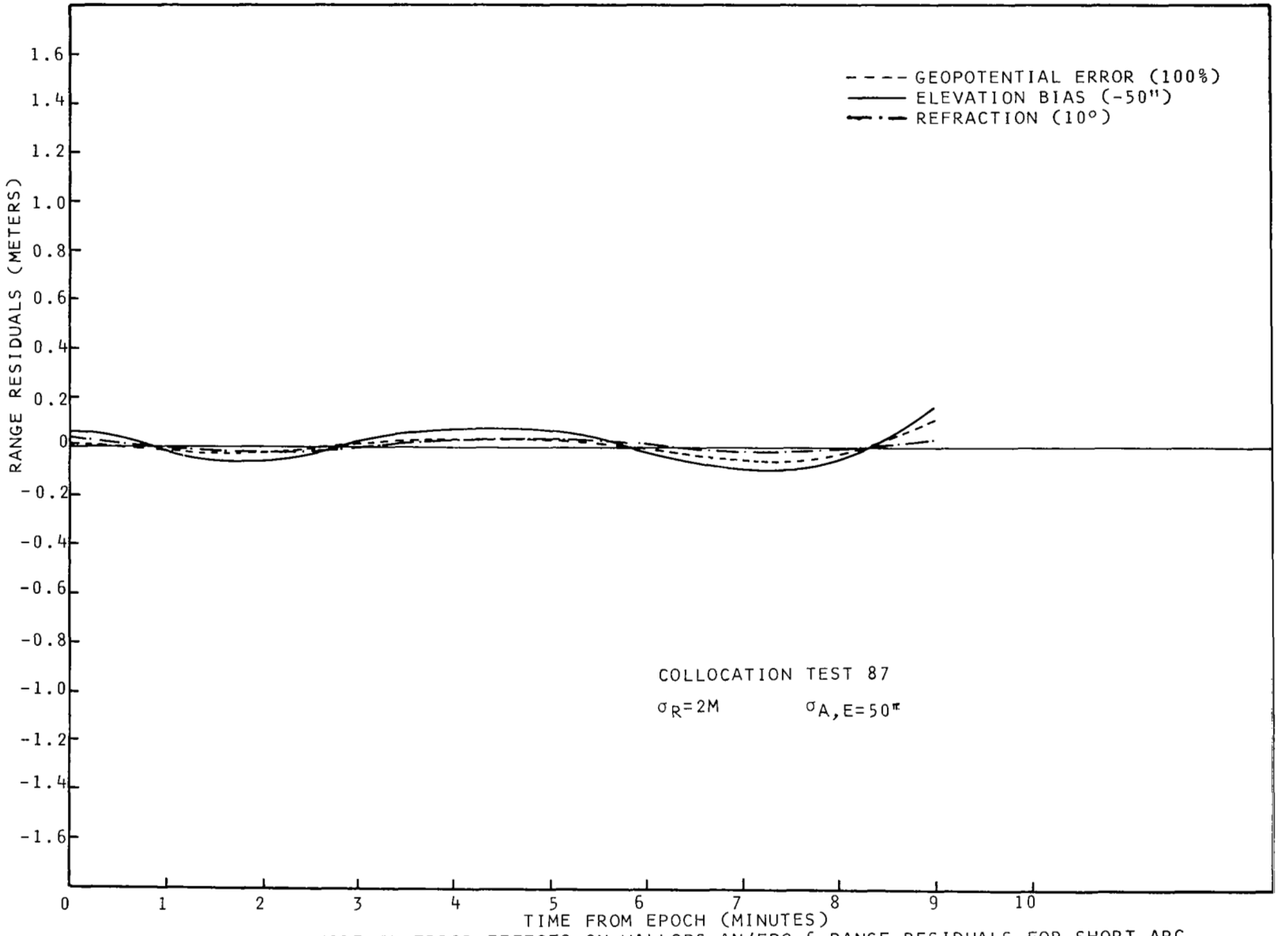

FIGURE 17 UNMODELED ERROR EFFECTS ON WALLOPS AN/FPQ-6 RANGE RESIDUALS FOR SHORT ARC

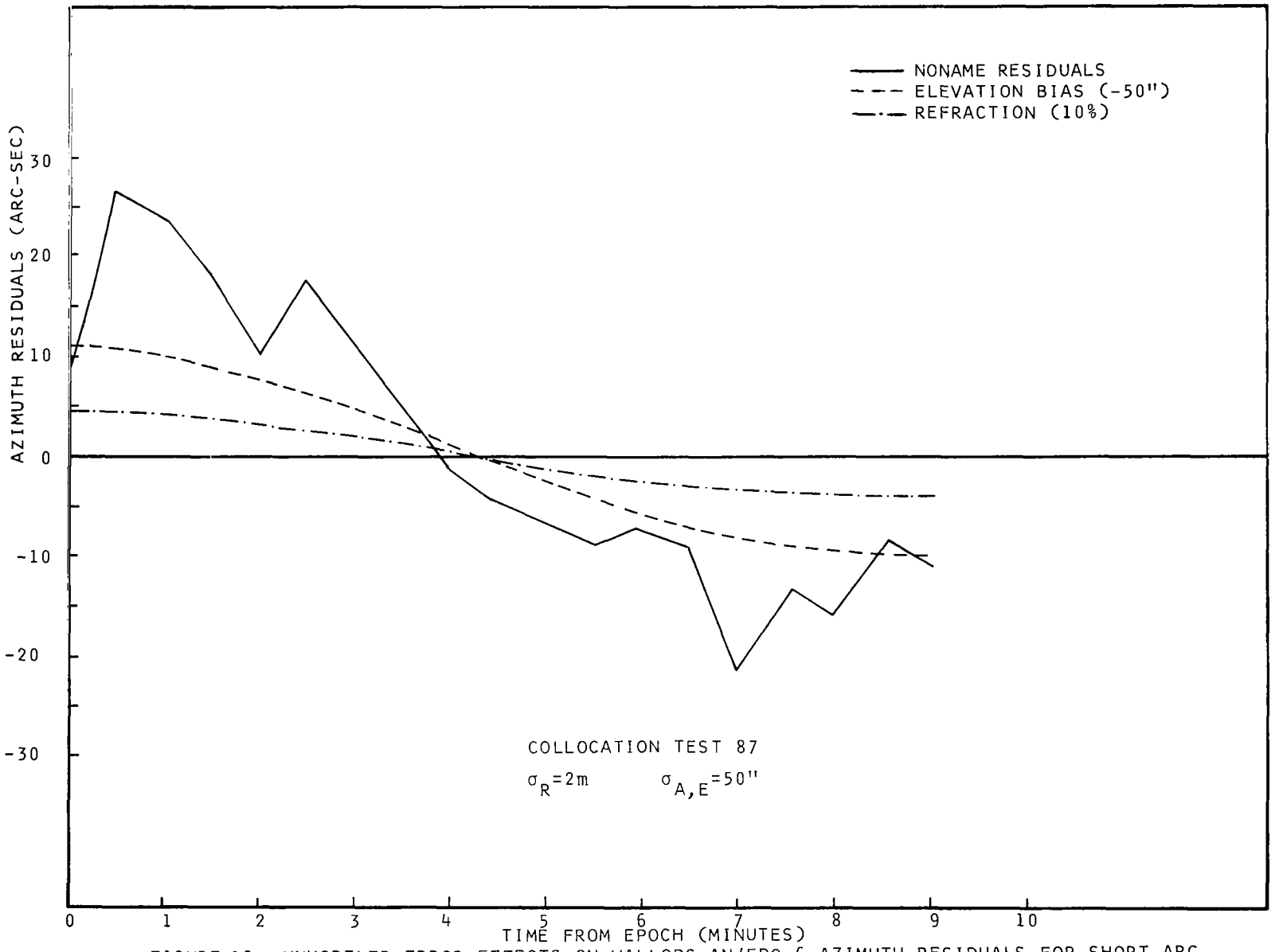

FIGURE 18 UNMODELED ERROR EFFECTS ON WALLOPS AN/FPQ-6 AZIMUTH RESIDUALS FOR SHORT ARC

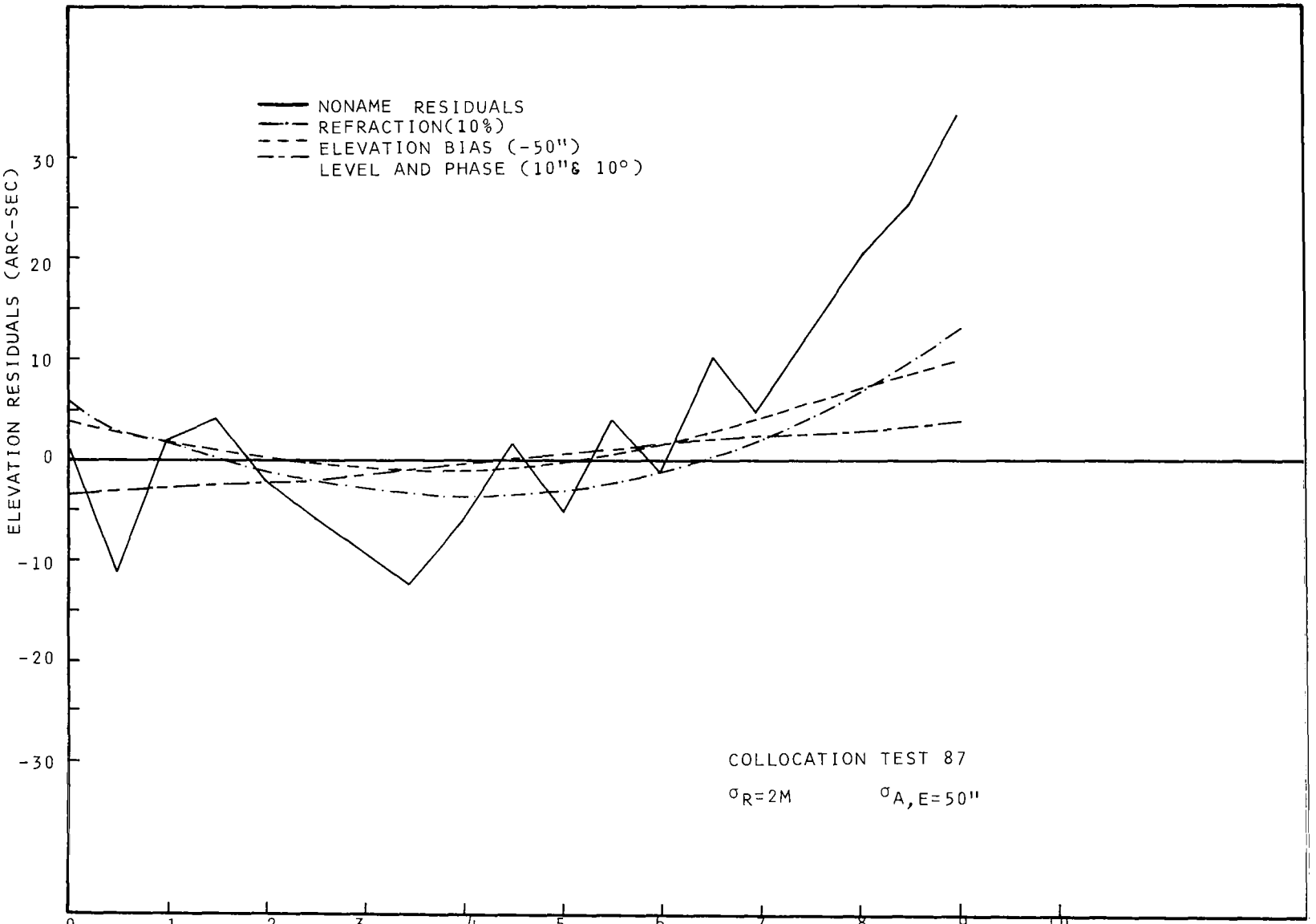

FIGURE 19 UNMODELED ERROR EFFECTS ON WALLOPS AN/FPQ-6 ELEVATION RESIDUALS FOR SHORT ARC

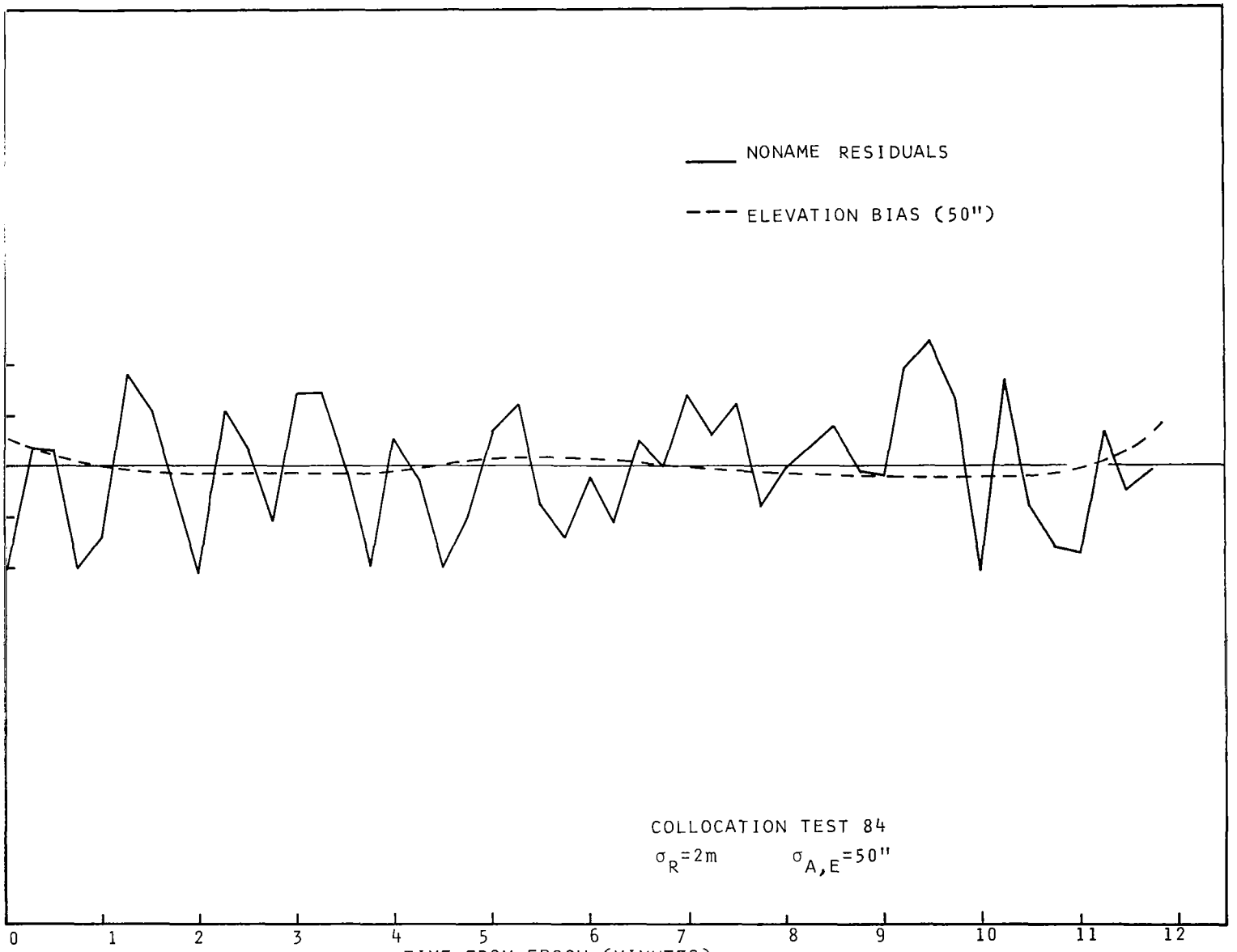

FIGURE 20 UNMODELED ERROR EFFECTS ON WALLOPS AN/FPQ-6 RESIDUALS FOR SHORT ARC

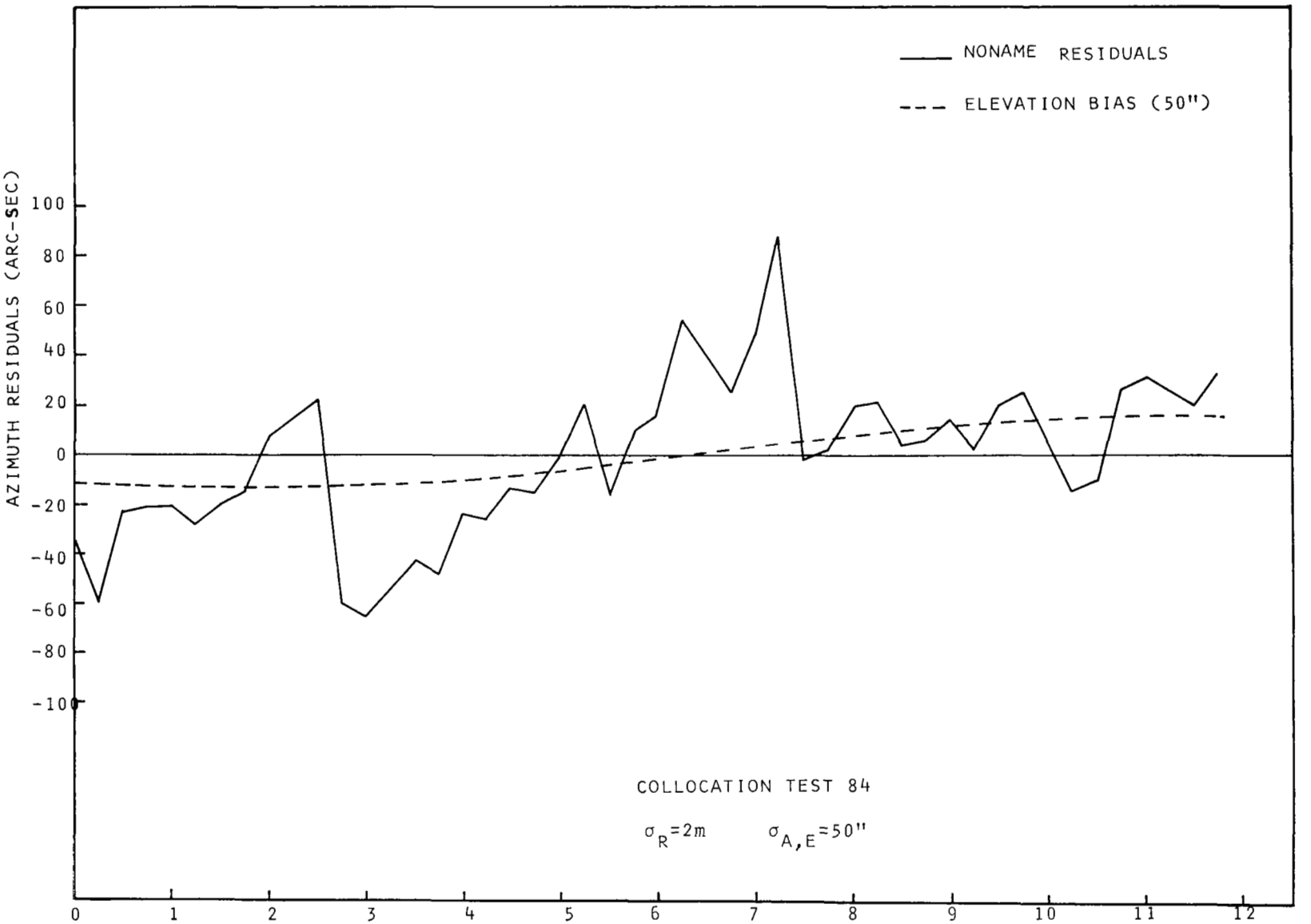

FIGURE 21 UNMODELED ERROR EFFECTS ON WALLOPS AN/FPQ-6 RESIDUALS FOR SHORT ARC

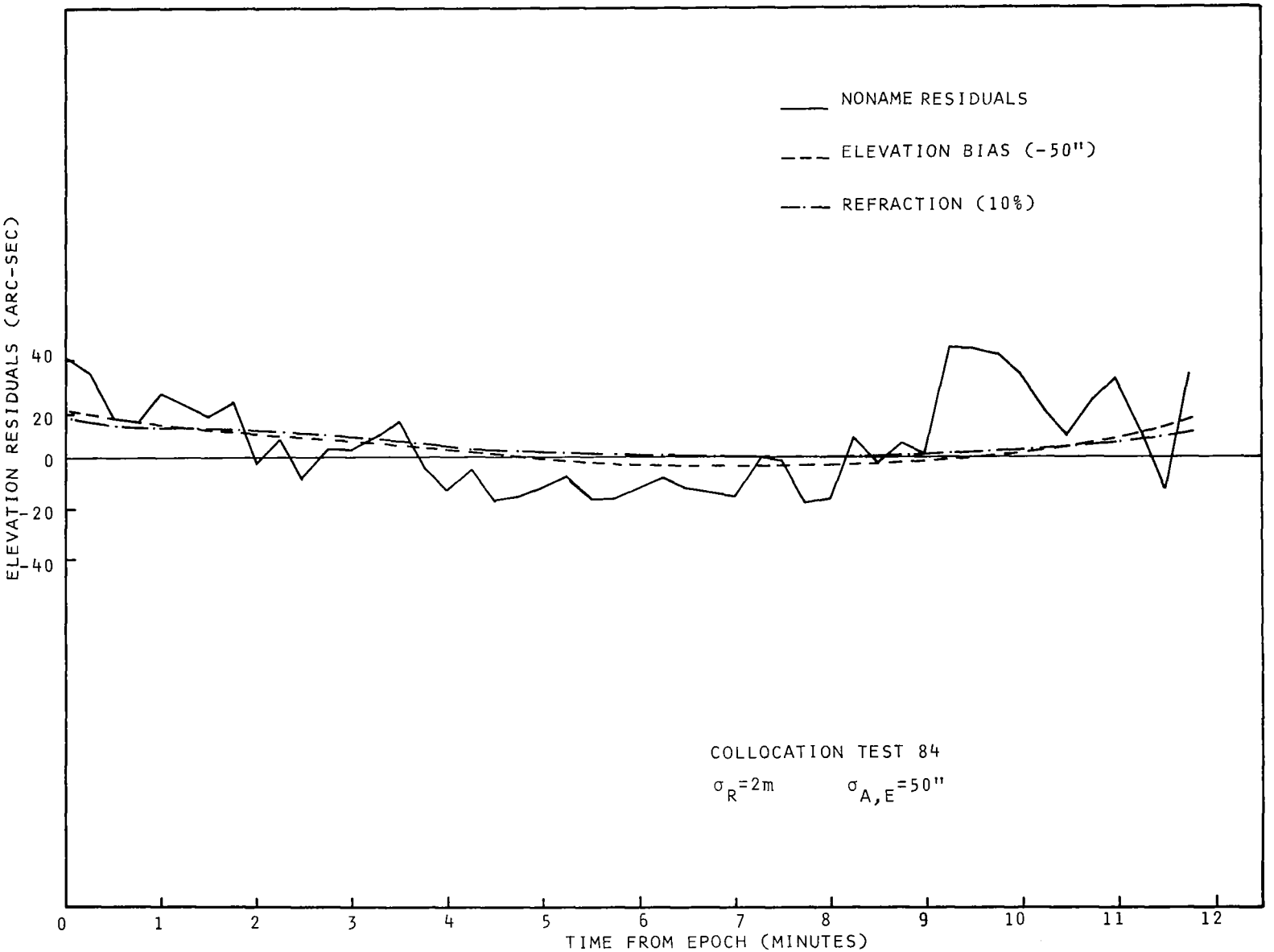

FIGURE 22 UNMODELED ERROR EFFECTS ON WALLOPS AN/FPQ-6 RESIDUALS FOR SHORT ARC

error effects are shown on the graphs. The NONAME residuals are superimposed on each graph for comparison.

Because the range residuals are essentially random for both cases, no explanation is required for its behavior pattern although very slight systematic errors are evident. However comparison of the actual angle residuals with the unmodeled errors show that a negative elevation bias of 50 arc - sec coupled with a positive 10% refraction error adequately describes the gross features of the actual angle tracking residuals. As previously demonstrated (see Section 4), the systematic errors are, to a large extent, absorbed by the orbit for single radar short arc solutions. This explains the lack of larger unmodeled error effects on the measurement residuals.

Although it is difficult to make any general conclusions regarding the explanation of all systematic trends experienced by radar tracking systems, this analysis does demonstrate the effectiveness of using unmodeled systematic errors as unadjusted parameters for studying trends in the AN/FPQ-6 radar measurement residuals over a short arc.

7.2 LARGE LONG ARC MEASUREMENT RESIDUALS

In Sections 4.2, 5.2, and 6.3, we always came to the conclusion that the most significant source of error in multi-revolution orbital solutions consisted of errors in the geopotential model. It would therefore be desirable to demonstrate that this conclusion is consistent with actual data reductions.

For all error sources which the ORAN program considers,

there is a well defined error model with the exception of geopotential coefficient errors. The only uncertainty in the total error produced by the error source is that due to uncertainty in the value of the coefficient of the error model term. For variance computation purposes, the coefficient of the error model term is a random variable, but the effect which the error has on an orbital solution is completely deterministic except for sign and amplitude.

In the case of geopotential coefficient errors, even the form of the error model term is a random variable (at least when all geopotential coefficient errors are lumped together, and this is the only case which will be considered here). The gravity model difference technique which we are employing to model geopotential errors is expected to generally produce the appropriate error amplitudes, but never anything such as the shape of a residual.

In Figure 24, we show the actual residuals from a NONAME data reduction for a Wallops FPQ-6 only 48 hour arc. In Figure 23, we show the ORAN computed effects on this data reduction (using the same data spans and the same measurement weights) of geopotential coefficient errors modeled by 40% of the difference between the SAO M1 and the Applied Physics Lab. 3.5 gravity models. Only 40% of the difference was used because the data reduction used the SAO model which is considered to be the more accurate. The actual figure of 40% was rather arbitrary.

It will be noted by comparing Figures 23 and 24 that they indeed do have residuals of approximately the same magnitude, although the shapes, as should be expected, are not very similar. We can therefore conclude that the ORAN computations are at least consistent with what is observed from actual data reductions. Large residuals from long arc data reductions are primarily attributable to errors in the gravity model used.

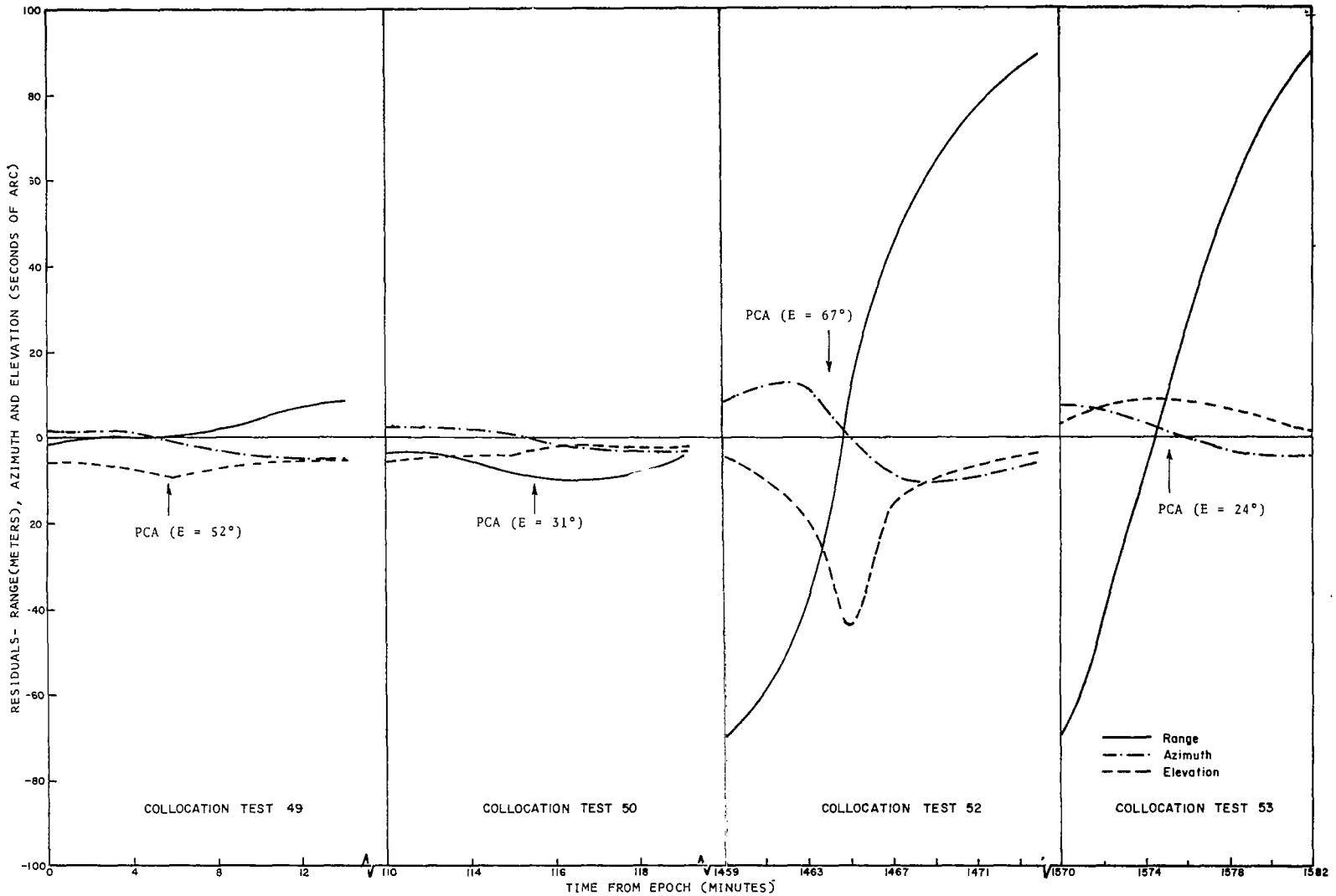

FIGURE 23 MAJOR UNMODELED ERROR EFFECTS ON WALLOPS ISLAND AN/FPQ-6 RESIDUALS DUE TO APL-SAO GRAVITY MODEL DIFFERENCES ON LONG ARC SOLUTION

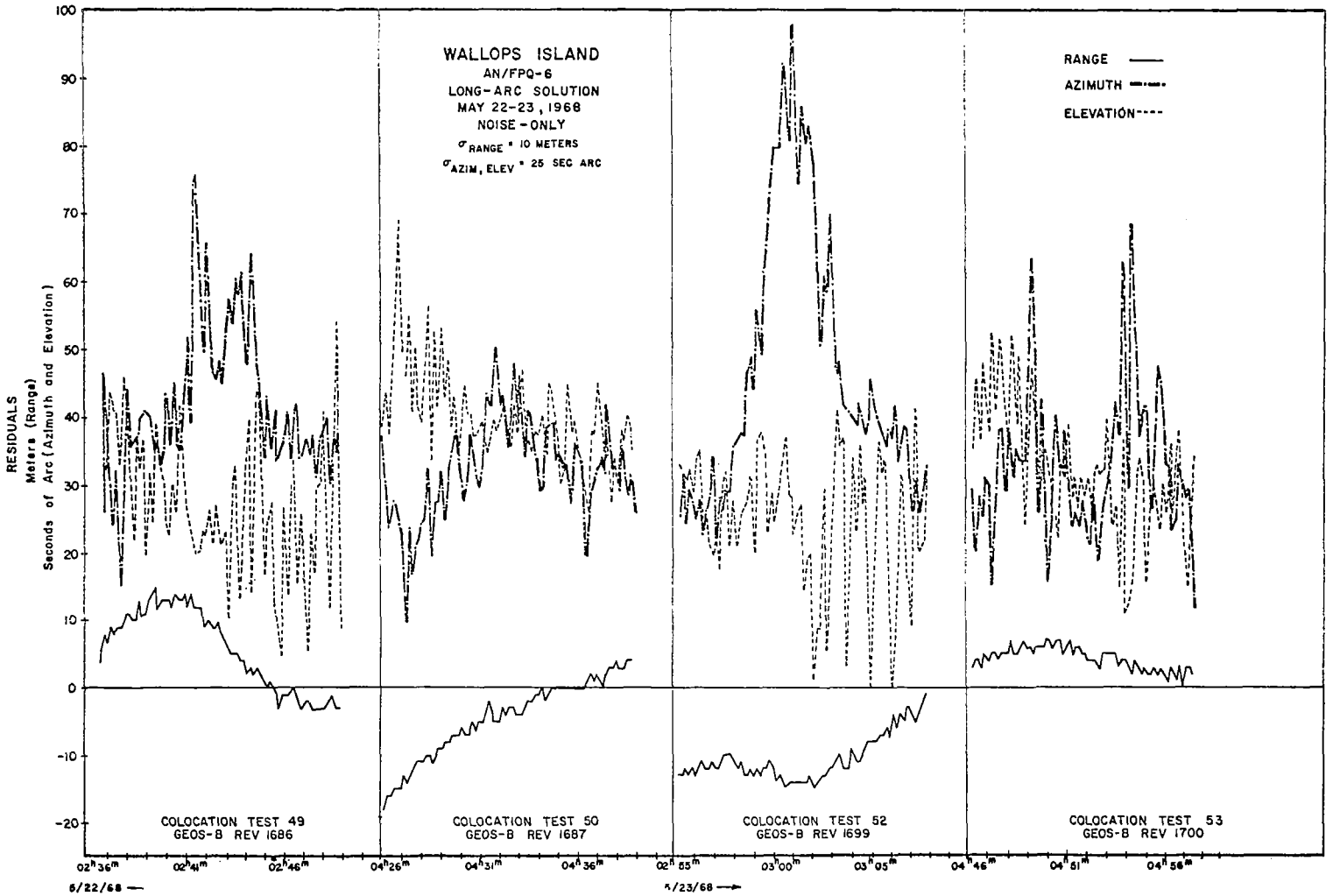
WALLOPS ISLAND
AN/FPQ-6
LONG-ARC SOLUTION
MAY 22-23, 1968
NOISE-ONLY
σ RANGE = 10 METERS
σ AZIM, ELEV = 25 SEC ARC
RANGE
AZIMUTH
ELEVATION
RESIDUALS
Meters (Range)
Seconds of Arc (Azimuth and Elevation)
100
90
80
70
60
50
40
30
20
10
0
-10
-20
COLOCATION TEST 49
GEOS-B REV 1686
COLOCATION TEST 50
GEOS-B REV 1687
COLOCATION TEST 52
GEOS-B REV 1699
COLOCATION TEST 53
GEOS-B REV 1700
02h36m
02h41m
02h46m
04h26m
04h31m
04h36m
02h55m
03h00m
03h05m
04h46m
04h51m
04h56m
5/22/68
5/23/68

Figure 24

SECTION 8.0
CONCLUSIONS

In this report an attempt has been made to demonstrate various characteristics of orbital solutions using data from one or more FPQ-6 radars. All computations were made using the ORAN program, which simulates the data reduction process in all essential respects and calculates the effects on the whole process of the presence of certain systematic errors. These errors always exist to some extent, but their effects depend greatly upon the tracking configuration and the length of the arc. The consideration of the effects of unmodeled errors in a number of situations leads to the following general conclusions:

a. Short arc single station orbital solutions are seriously affected by systematic measurement errors. That is, the measurement errors get propagated into the orbit, and may be only slightly evident in the measurement residuals. There is a very limited capability for any error model recovery.

b. Multi-station short arcs have a significant potential for error model recovery with favorable tracking geometry.

c. Long arc multi-station solutions can be used for radar angle calibration and, to some extent, to estimate other parameters. The largest effects on calibration uncertainties are geopotential and refraction errors.

d. Long arc solutions by FPQ-6 radars are essentially determined by the range and range rate measurements. Systematic angle measurement errors thus do not get propagated into the orbit and show up in the residuals.

e. Geopotential coefficient errors constitute the largest deterrent to accuracy of long arc solutions.

APPENDIX A

ORAN MATHEMATICS

SECTION A1
INTRODUCTION

The assumptions inherent in the least squares orbital solution are never completely satisfied, primarily because of various systematic errors existing in the measurements and force model. Various procedures can be used to minimize these errors such as careful data preprocessing, use of the best available set of geopotential coefficients, inclusion of all significant perturbative forces, and recovery of certain error model parameters. However, the number of error model parameters which can be successfully recovered is limited by computer storage and running time considerations, as well as the information contained in the data itself. Furthermore, there are limitations in our knowledge of the most significant parameters and on our ability to model certain types of errors, particularly force model errors.

It follows that the assumptions underlying the least squares orbital solution can never be completely satisfied. As a corollary, this means that solution accuracy estimates which assume that all systematic effects have been modeled will give overly optimistic error estimates.

We can calculate realistic estimates of the accuracy of a least squares orbital solution, provided that error estimates for the ignored parameters are available As a by-product of this calculation, the effects on the orbital solution of each individual error model term are available. The latter may be used to identify the importance of various error source on a particular solution.

The mathematics discussed have been implemented in an ORbital ANalysis (ORAN) computer program of considerable complexity. A wide variety of error model terms may be considered, and the program can consider errors which arise when multiple satellite arcs are processed simultaneously for the recovery of geopotential, station position, and other parameters.

SECTION A2

ADJUSTED BIAS PARAMETERS

The main purpose of the ORAN program is to calculate effects on an orbital determination, and/or instrumentation calibration, of the lack of validity of certain assumptions made in the minimum variance type reduction of orbital tracking data. In particular, the effects of ignoring the presence of various systematic errors are calculated. Because of several partitionings involved in the matrix inversions, the mathematics of the ORAN program becomes somewhat involved. The following development gives the mathematics used by the ORAN program, but does not, in general, specify the order in which the operations are performed.

Consider first the propagation of unmodeled error effects into the bias parameters and orbital elements determined for a single arc. The trajectory measurements may be related to the orbital elements and biases by the matrix equation

$$(m)_{nm \times 1} = (A)_{nm \times 6}(a)_{6 \times 1} + (K)_{nm \times na}(k)_{na \times 1}$$

$$+ (B)_{nm \times nu}(\gamma)_{nu \times 1} + (\varepsilon)_{nm \times 1} \quad , \qquad 2\text{-}1$$

where the symbols have the meanings:

m - a column vector representing the deviation of the actual measurement from that for some approximate orbit (m is sometimes called the discrepancy vector).

A - a matrix giving the partial derivatives of the measurements with respect to the epoch orbital elements, evaluated on the approximate orbit.

a - a column vector representing the deviation of the true orbital elements at epoch from those for the approximate orbit. Orbital elements in the ORAN program are inertial Cartesian.

K - a matrix giving the partial derivatives of the measurements with respect to those bias parameters which are considered to be adjusted.

k - deviations of the adjusted parameters from their approximate (or a priori) values.

B - same as K except with respect to parameters which are not to be adjusted.

γ - same as k except referring to parameters which are not to be adjusted.

ε - a column vector representing the random noise on the measurements.

nm - total number of measurements.

nea - number of adjustable bias parameters.

nu - number of unadjusted bias parameters.

With γ known, the minimum variance solution of Equation 2-1 for a and k is

$$\begin{bmatrix} \hat{a} \\ \hat{k} \end{bmatrix} = \begin{bmatrix} A^T W A & A^T W K \\ K^T W A & K^T W K \end{bmatrix}^{-1} \begin{bmatrix} A^T W \\ K^T W \end{bmatrix} (m - B\gamma) \qquad 2\text{-}2$$

$$= \begin{bmatrix} M_a & M_{ak} \\ M_{ak}^T & M_k \end{bmatrix} \begin{bmatrix} A^T W \\ K^T W \end{bmatrix} (m - B\gamma) \ , \qquad 2\text{-}3$$

where

$$W^{-1} = E(\epsilon \ \epsilon^T) \qquad 2\text{-}4$$

$$M_k = \left[K^T W K - K^T W A (A^T W A)^{-1} A^T W K \right]^{-1} \qquad 2\text{-}5$$

$$M_{ak} = -QM_k, \text{ with } Q = (A^T WA)^{-1} A^T WK \qquad 2\text{-}6$$

$$M_a = (A^T WA)^{-1} + QM_k Q^T \qquad 2\text{-}7$$

The variances of these estimates, neglecting the unmodeled parameters, are given by

$$\text{Var}(\hat{a})_{mod} = M_a \qquad 2\text{-}8a$$

$$\text{Var}(\hat{k})_{mod} = M_k , \qquad 2\text{-}8b$$

and the covariance is given by

$$\text{Cov}(\hat{a}\,\hat{k}^T)_{mod} = M_{ak}. \qquad 2\text{-}8c$$

The unadjusted parameter contribution to the total variance will be computed below.

To see how the solution given by Equation 2-3 differs for different assumed values of γ, the equation may be differentiated with respect to γ to give

$$\frac{\partial \hat{a}}{\partial \gamma} = -M_a A^T W B - M_{ak} K^T W B \qquad 2\text{-}9$$

$$\frac{\partial \hat{k}}{\partial \gamma} = -M_{ak}^T A^T W B - M_k K^T W B. \qquad 2\text{-}10$$

Using Equations 2-6, 2-7, and 2-9 . Equation 2-10 may be re-written in the more convenient form

$$\frac{\partial \hat{a}}{\partial \gamma} = -(A^T W A)^{-1} \left[A^T W B + A^T W K \frac{\partial \hat{k}}{\partial \gamma}\right] \qquad 2\text{-}11$$

As such, the ORAN program does not compute the total variance of the $\hat{a}$ estimate. To see the expression which should be used to compute the total variance of $\hat{k}$, compute the expected value

$$\text{Var}\,\hat{k} = E(\hat{k}\,\hat{k}^T)$$

$$= E\left\{ [M_{ak}^T A^T W + M_k K^T W] \; (m - B\gamma) \; (m - B\gamma)^T \right.$$

$$\left. x [M_{ak}^T A^T W + M_k K^T W]^T \right\}. \qquad 2\text{-}12$$

Assuming

$$E(m\ m^T) = E(\varepsilon\ \varepsilon^T) = W^{-1},$$

$$E(m\ \gamma^T) = 0$$

$$E(\gamma\ \gamma^T) = \text{Var}\ \gamma\ , \qquad 2\text{-}13$$

Then Equation 2-12 may be written

$$\text{Var}\ \hat{k} = (M_{ak}^T A^T + M_k K^T)(M_{ak}^T A^T W + M_k K^T W)^T$$

$$+ (M_{ak}^T A^T WB + M_k K^T WB)\text{Var}\ \gamma (M_{ak}^T A^T WB + M_k K^T WB)^T$$

$$= M_k + \frac{\partial \hat{k}}{\partial \gamma}\ \text{Var}\ \gamma\ \left(\frac{\partial \hat{k}}{\partial \gamma}\right)^T, \qquad 2\text{-}14$$

as may be verified by the use of Equations 2-5, 2-6, 2-10, and a little matrix algebra.

SECTION A3
EFFECTS OF UNMODELED PARAMETER ERRORS ON ORBITAL ACCURACY

At any time the deviations of the orbital estimate using the estimated $\hat{a}$ and $\hat{k}$, from the approximate values may be expressed as

$$(\hat{x})_{6 \times 1} = (\tilde{A})_{6 \times 6}(\hat{a})_{6 \times 1} + (G)_{6 \times na}(\hat{k})_{na \times 1} + (H)_{6 \times nu}(\gamma)_{nu \times 1} \quad , \qquad 3\text{-}1$$

where the symbols have the meanings:

$\hat{x}$ - corrections applied to the orbit from the previous approximation, or iteration.

$\tilde{A}$ - the "dynamic partials" of the orbit at any point with respect to the set of 6 epoch elements.

G - the partials of the orbit with respect to the set of adjusted error model terms. Note that in general this matrix can have non-zero columns only for geopotential and drag parameters.

$\hat{a}$ - adjustments of the orbital elements from their approximate values.

$\hat{k}$ - adjustments of modeled parameters from their approximate values.

H - the partials of the orbit with respect to the set of unadjusted error model terms. This matrix also has non-zero columns only for geopotential and drag type parameters.

γ - deviations of the true values of the unmodeled parameter set from their assumed values.

Unit errors in γ thus lead to effects on the orbit of

$$\frac{\partial \hat{x}}{\partial \gamma} = \tilde{A} \frac{\partial \hat{a}}{\partial \gamma} + G \frac{\partial \hat{k}}{\partial \gamma} + H. \qquad 3\text{-}2$$

To obtain the variance of the estimated $\hat{x}$, Equation 3-1 may first be rewritten, using Equation 2-3 as

$$\hat{x} = \left[\tilde{A} \mid G\right] \begin{bmatrix} M_a & M_{ak} \\ M_{ak}^T & M_k \end{bmatrix} \begin{bmatrix} A^T W \\ K^T W \end{bmatrix} (m - B\gamma) + H\gamma.$$

Making use of Equations 2-9, 2-10, and 3-2 we can also write $\hat{x}$ as:

$$\hat{x} = [\tilde{A} \mid G] \begin{bmatrix} M_a & M_{ak} \\ M_{ak}^T & M_k \end{bmatrix} \begin{bmatrix} A^T W \\ K^T W \end{bmatrix} .m + \frac{\partial \hat{x}}{\partial \gamma} \gamma \qquad 3\text{-}3$$

Next using the definition of the variance of $\hat{x}$,

$$\text{Var}(\hat{x}) = E(\hat{x}\,\hat{x}^T)$$

$$= E\left\{ [\tilde{A} \mid G] \begin{bmatrix} M_a & M_{ak} \\ M_{ak}^T & M_k \end{bmatrix} \begin{bmatrix} A^T W \\ K^T W \end{bmatrix} m + \frac{\partial \hat{x}}{\partial \gamma} \gamma \right\}$$

$$x \left\{ [\tilde{A} \mid G] \begin{bmatrix} M_a & M_{ak} \\ M_{ak}^T & M_k \end{bmatrix} \begin{bmatrix} A^T W \\ K^T W \end{bmatrix} m + \frac{\partial \hat{x}}{\partial \gamma} \gamma \right\}^T ,$$

and again making the assumptions on m and γ as expressed by Equation 2-13

$$\mathrm{Var}(x) = \left[\tilde{A} \mid G\right] \left[\begin{array}{c|c} M_a & M_{ak} \\ \hline M_{ak}^T & M_k \end{array}\right] \left[\begin{array}{c} \tilde{A}^T \\ \hline G^T \end{array}\right] + \left(\frac{\partial \hat{x}}{\partial \gamma}\right) \mathrm{Var}\,\gamma \left(\frac{\partial \hat{x}}{\partial \gamma}\right)^T . \qquad 3\text{-}4$$

The form of the final result of Equation 3-4 is thus exactly the expected form, namely the standard form for the contribution due to the modeled parameters and an unadjusted parameter contribution which may be written in terms of partial derivatives in the same way as was done for Var k in Equation 2-14.

SECTION A4
PARTITIONING OF ADJUSTED PARAMETER SET

Now suppose that the parameter sets k and γ are partitioned into the sets (k_o, γ_o), (k_1, γ_1), ... , (k_n, γ_n), where the (k_o, γ_o) parameters are common to all arcs, and the (k_i, γ_i) parameters affect only the i^{th} arc. The M_k matrix is still given by Equation 2-5. For simplicity, let n = 1. M_k may then be written

$$M_k = \left\{ \left[\begin{array}{c|c} K_o^T W K_o & K_o^T W K_1 \\ \hline K_1^T W K_o & K_1^T W K_1 \end{array}\right] - \left[\begin{array}{c} K_o^T W A \\ \\ K_1^T W A \end{array}\right] (A^T W A)^{-1} \left[\begin{array}{c} K_o^T W A \\ \\ K_1^T W A \end{array}\right]^T \right\}^{-1} . \qquad 4\text{-}1$$

It is convenient to denote this as

$$M_k = \left[\begin{array}{cc} \left\{K_o^T W K_o\right\} & \left\{K_o^T W K_1\right\} \\ \\ \left\{K_1^T W K_o\right\} & \left\{K_1^T W K_1\right\} \end{array}\right]^{-1} = \left[\begin{array}{cc} M_o & M_{o1} \\ \\ M_{o1}^T & M_1 \end{array}\right] , \qquad 4\text{-}2$$

where

$$\left\{K_o^T W K_o\right\} \equiv K_o^T W K_o - K_o^T W A (A^T W A)^{-1} (K_o^T W A)^T \qquad 4\text{-}3$$

$$\left\{K_o^T W K_1\right\} \equiv K_o^T W K_1 - K_o^T W A (A^T W A)^{-1} (K_1^T W A)^T \qquad 4\text{-}4$$

$$\left\{K_1^T W K_1\right\} \equiv K_1^T W K_1 - K_1^T W A (A^T W A)^{-1} (K_1^T W A)^T \qquad 4\text{-}5$$

$$M_o \equiv \left[\left\{K_o^T W K_o\right\} - \left\{K_o^T W K_1\right\} \left\{K_1^T W K_1\right\}^{-1} \left\{K_o^T W K_1\right\}^T\right]^{-1} \qquad 4\text{-}6$$

$$M_{o1} = -M_o Q_{1o}^T, \quad Q_{1o} = \left\{K_1^T W K_1\right\}^{-1} \left\{K_1^T W K_o\right\} \qquad 4\text{-}7$$

$$M_1 = \left\{K_1^T W K_1\right\}^{-1} + Q_{1o} M_o Q_{1o}^T \quad . \qquad 4\text{-}8$$

Note that the same partitioning algorithm used in going from Equation 2-2 to Equation 2-3 can be used in inverting Equation 4-2.

The derivatives of the adjusted parameters with respect to the unadjusted parameters can be found by substituting into the general expression, Equation 2-10,

$$\frac{\partial \hat{k}}{\partial \gamma} = +M_k (K^T W A)(A^T W A)^{-1} (A^T W B) - M_k K^T W B \quad ,$$

or

$$\frac{\partial \hat{k}}{\partial \gamma} = -\left[\begin{array}{c|c} M_o & M_{o1} \\ \hline M_{o1}^T & M_1 \end{array}\right]\left[\begin{pmatrix} K_o^T W B \\ \\ K_1^T W B \end{pmatrix} - \begin{pmatrix} K_o^T W A \\ \\ K_1^T W A \end{pmatrix}(A^T W A)^{-1} (A^T W B)\right]$$

$$= -\left[\begin{array}{c|c} M_o & M_{o1} \\ \hline M_{o1}^T & M_1 \end{array}\right]\left[\begin{matrix} \left\{K_o^T W B\right\} \\ \\ \left\{K_1^T W B\right\} \end{matrix}\right] \quad . \qquad 4\text{-}9$$

Substituting for M_o, M_{o1}, and M_1 from Equations 4-6 through 4-8 it follows that the parameter derivatives may be expressed as

$$\frac{\partial \hat{k}_o}{\partial \gamma} = -M_o\left[\left\{K_o^T WB\right\} - \left\{K_o^T WK_1\right\}\left\{K_1^T WK_1\right\}^{-1}\left\{K_1^T WB\right\}\right] \qquad 4\text{-}10$$

$$\frac{\partial \hat{k}_1}{\partial \gamma} = +\left\{K_1^T WK_1\right\}^{-1}\left\{K_1^T WK_o\right\} M_o \left\{K_o^T WB\right\}$$

$$- \left[\left\{K_1^T WK_1\right\}^{-1} + \left\{K_1^T WK_1\right\}^{-1}\left\{K_1^T WK_o\right\} M_o \left\{K_1^T WK_o\right\}^T\right.$$

$$\left. x \left\{K_1^T WK_1\right\}^{-1}\right]\left\{K_1^T WB\right\}$$

$$= -\left\{K_1^T WK_1\right\}^{-1}\left[\left\{K_1^T WB + \left\{K_1^T WK_o\right\}\frac{\partial \hat{k}_o}{\partial \gamma}\right]\right. . \qquad 4\text{-}11$$

This result is exactly analogous to that expressed by Equation 2-11.

SECTION A5
MEASUREMENT RESIDUALS

From Equation 2-1, the residual which will remain after a and k have been estimated is given by

$$e = m - A\hat{a} - K\hat{k} - B\gamma. \qquad 5\text{-}1$$

Again differentiation with respect to γ,

$$\frac{\partial e}{\partial \gamma} = -A \frac{\partial \hat{a}}{\partial \gamma} - K \frac{\partial \hat{k}}{\partial \gamma} - B, \qquad 5\text{-}2$$

shows the effects of unit values of the unadjusted parameters. For any measurement, the residual derivatives with respect to the unadjusted parameter set, and scaled by the a priori sigmas of these parameters, are an optional output; measurement rate derivatives are output only if only the rate data from the measurement are being used.

APPENDIX B
TYPICAL GEOS II MEASUREMENT RATE AND ACCELERATION PROFILES FROM WALLOPS FPQ-6 RADAR

The ORAN program was simulated in a mode to compute typical range, azimuth and elevation measurement profiles as observed by the Wallops Island AN/FPQ-6 radar. Figure B-1 illustrates these profiles for a low elevation pass configuration over Wallops; similarly Figure B-2 illustrates the profiles for a high elevation pass configuration.

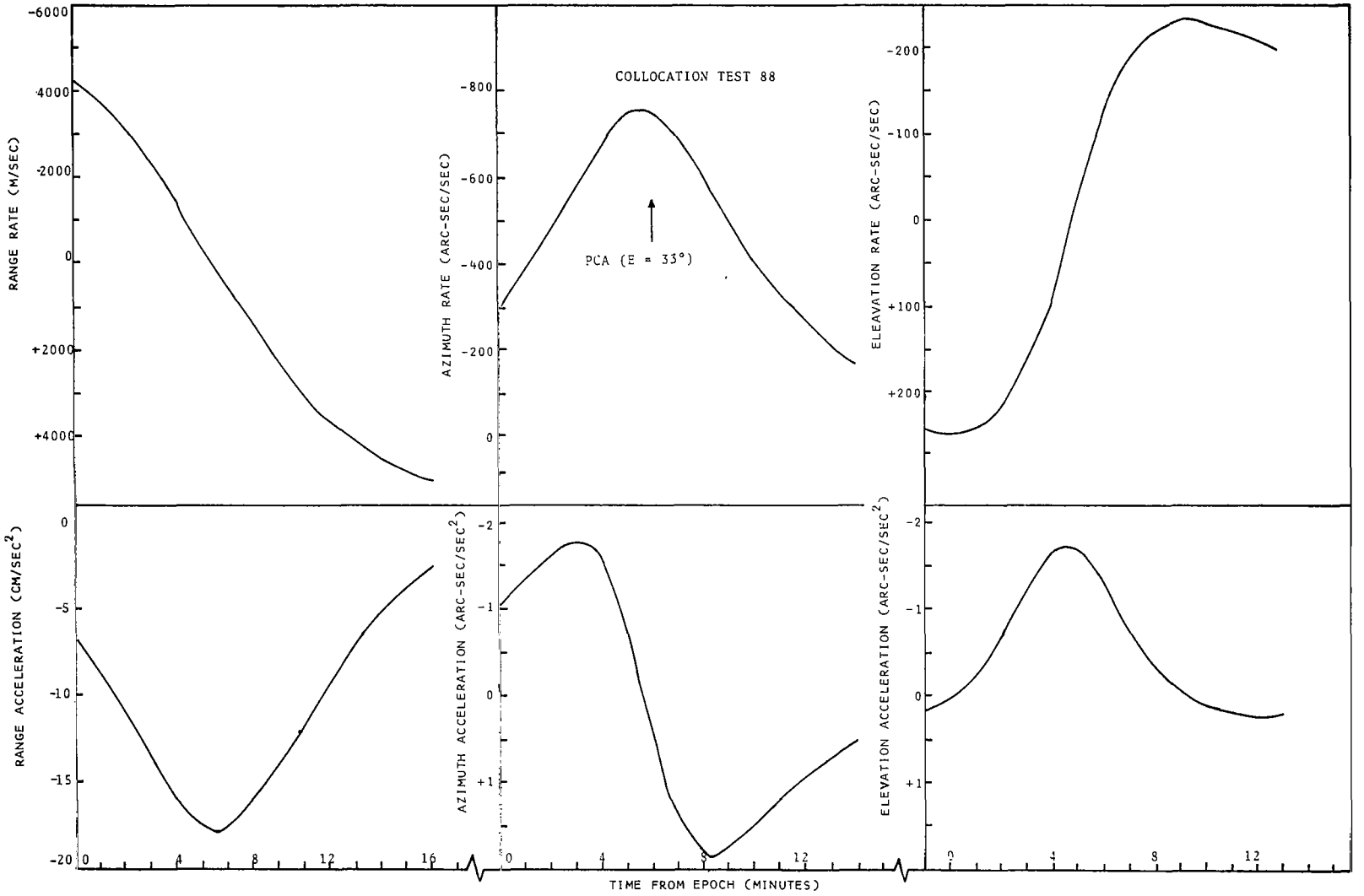

FIGURE B-1 TYPICAL GEOS II RATE AND ACCELERATION MEASUREMENTS FROM WALLOPS AN/FPQ-6 RADAR

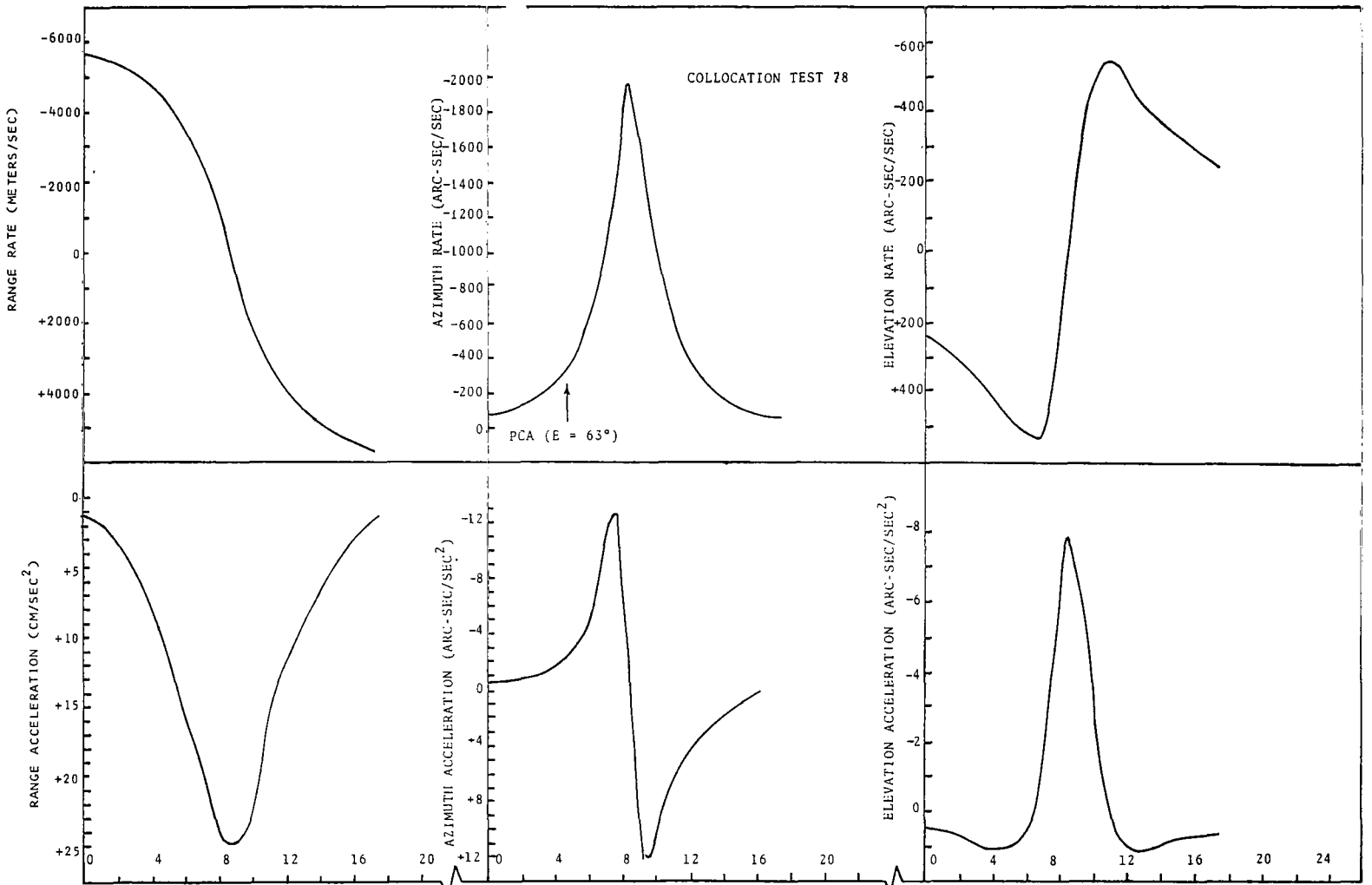

FIGURE B-2
TYPICAL GEOS-II RATE AND ACCELERATION MEASUREMENTS FROM WALLOPS ISLAND AN/FPQ-6 RADAR

REFERENCES

1. Martin, C.E., Carroll Jr., C.A., Tropospheric Refraction Corrections and their Residual Errors, AFMTR-TDR-64-3, Feb. 1965.

2. Lundquist, C.A., Veis, G., Geodetic Parameters for a 1966 Smithsonian Institution Standard Earth, SAO Special Report No. 200, 1966.

3. Veis, G., A Comparison of Station Positions Obtained from Photographic and Radio Tracking Data, SAO Report, Oct. 1966.

4. Whipple, F.L., Veis, G., Gaposchkin, E.M., Kohnlein, W. and Strange, W.E., "Geodetic Parameters for a Standard Earth Obtained from Baker-Nunn Observations," Presented at 7th COSPAR Mtg., Vienna, May 1966.

5. Sjogren, W.L., Trask, D.W., Vegos, C.J., Wollenhaupt, W.R., "Physical Constants as Determined from Radio Tracking of the Ranger Lunar Probes," AAS Preprint No. 66-105, July 1966.

NASA-Langley, 1970 —— 30 CR-1511